PD ISO/TS 20459:2023

BSI Standards Publication

Road vehicles — Injury risk functions for advanced pedestrian legform impactor (aPLI)

Documents
Document Sharing Hub

Full document details: PD ISO/TS 20459:2023

National foreword

This Published Document is the UK implementation of ISO/TS 20459:2023.

The UK participation in its preparation was entrusted to Technical Committee AUE/7, Automobile occupant restraint systems.

A list of organizations represented on this committee can be obtained on request to its committee manager.

Contractual and legal considerations

This publication has been prepared in good faith, however no representation, warranty, assurance or undertaking (express or implied) is or will be made, and no responsibility or liability is or will be accepted by BSI in relation to the adequacy, accuracy, completeness or reasonableness of this publication. All and any such responsibility and liability is expressly disclaimed to the full extent permitted by the law.

This publication is provided as is, and is to be used at the recipient's own risk.

The recipient is advised to consider seeking professional guidance with respect to its use of this publication.

This publication is not intended to constitute a contract. Users are responsible for its correct application.

This publication is not to be regarded as a British Standard.

© The British Standards Institution 2023
Published by BSI Standards Limited 2023

ISBN 978 0 539 16688 0

ICS 43.020

Compliance with a Published Document cannot confer immunity from legal obligations.

This Published Document was published under the authority of the Standards Policy and Strategy Committee on 31 May 2023.

Amendments/corrigenda issued since publication

Date	Text affected

Documents
Document Sharing Hub

TECHNICAL SPECIFICATION

ISO/TS 20459

First edition
2023-04

Road vehicles — Injury risk functions for advanced pedestrian legform impactor (aPLI)

Véhicules routiers — Critères lésionnels et courbes de risques pour l'impacteur en forme de jambe de piéton (aPLI).

Reference number
ISO/TS 20459:2023(E)

Documents
Document Sharing Hub

© ISO 2023

Full document details: PD ISO/TS 20459:2023

COPYRIGHT PROTECTED DOCUMENT

© ISO 2023

All rights reserved. Unless otherwise specified, or required in the context of its implementation, no part of this publication may be reproduced or utilized otherwise in any form or by any means, electronic or mechanical, including photocopying, or posting on the internet or an intranet, without prior written permission. Permission can be requested from either ISO at the address below or ISO's member body in the country of the requester.

ISO copyright office
CP 401 • Ch. de Blandonnet 8
CH-1214 Vernier, Geneva
Phone: +41 22 749 01 11
Email: copyright@iso.org
Website: www.iso.org

Published in Switzerland

© ISO 2023 – All rights reserved

Documents
Document Sharing Hub

Full document details: PD ISO/TS 20459:2023

Contents

Page

Foreword ..... **iv**
Introduction ..... **v**
1 Scope **1**
2 Normative references **1**
3 Terms and definitions **1**
4 Symbols and abbreviated terms **3**
4.1 Symbols 3
4.2 Abbreviated terms 4
5 IPFs for the aPLI **4**
5.1 General 4
5.2 Thigh 6
5.3 Leg 7
5.4 Knee 8
Annex A (informative) **Rationale regarding background and methodology to develop IPFs for the aPLI** **11**
Annex B (informative) **Adjustment of IPFs for real-world relevance** **105**
Annex C (informative) **Supplemental data** **135**
Annex D (informative) **Influence of PMHS test data (dfbetas > 0,3) against IPFs for human** **136**
Bibliography **154**

© ISO 2023 – All rights reserved

Documents
Document Sharing Hub
Full document details: PD ISO/TS 20459:2023

Foreword

ISO (the International Organization for Standardization) is a worldwide federation of national standards bodies (ISO member bodies). The work of preparing International Standards is normally carried out through ISO technical committees. Each member body interested in a subject for which a technical committee has been established has the right to be represented on that committee. International organizations, governmental and non-governmental, in liaison with ISO, also take part in the work. ISO collaborates closely with the International Electrotechnical Commission (IEC) on all matters of electrotechnical standardization.

The procedures used to develop this document and those intended for its further maintenance are described in the ISO/IEC Directives, Part 1. In particular, the different approval criteria needed for the different types of ISO documents should be noted. This document was drafted in accordance with the editorial rules of the ISO/IEC Directives, Part 2 (see www.iso.org/directives).

Attention is drawn to the possibility that some of the elements of this document may be the subject of patent rights. ISO shall not be held responsible for identifying any or all such patent rights. Details of any patent rights identified during the development of the document will be in the Introduction and/or on the ISO list of patent declarations received (see www.iso.org/patents).

Any trade name used in this document is information given for the convenience of users and does not constitute an endorsement.

For an explanation of the voluntary nature of standards, the meaning of ISO specific terms and expressions related to conformity assessment, as well as information about ISO's adherence to the World Trade Organization (WTO) principles in the Technical Barriers to Trade (TBT), see www.iso.org/iso/foreword.html.

This document was prepared by Technical Committee ISO/TC 22, *Road vehicles*, Subcommittee SC 36, *Safety and impact testing.*

Any feedback or questions on this document should be directed to the user's national standards body. A complete listing of these bodies can be found at www.iso.org/members.html.

© ISO 2023 – All rights reserved
Documents
Document Sharing Hub
Full document details: PD ISO/TS 20459:2023

Introduction

This document has been prepared on the basis of the existing injury probability functions (IPFs) to be used with the advanced pedestrian legform impactor (aPLI) standard build level B (SBL-B). The purpose of this document is to document the IPFs for the aPLI in a form suitable and intended for worldwide harmonized use.

In 2014, development of the aPLI hardware and associated IPFs started, with the aim of defining a globally accepted next-generation pedestrian legform impactor with enhanced biofidelity and injury assessment capability, along with its IPFs, suitable for harmonized use. Participating in the development were research institutes, dummy and instrumentation manufacturers, governments, and car manufacturers from around the world.

IPFs for the aPLI specified in this document predict injury probability to specific regions of the lower limb of a pedestrian that corresponds to maximum values of injury metrics obtained by the aPLI in a subsystem test, as described in References [1] and [2]. As the IPFs do not provide any threshold values, users will need to determine target injury probability, based on their specific needs, to define injury assessment reference values to be used for their test protocol.

It is also important to note that the subsystem test procedure (STP) for pedestrian protection may not be representative of pedestrian accidents for specific injury metrics, depending on their sensitivity to pedestrian impact conditions such as lower-limb posture and muscle tone. The IPFs for the aPLI have been validated against accident data and some ideas to compensate for the discrepancy against accident data are presented in Annex B.

© ISO 2023 – All rights reserved

Documents
Document Sharing Hub
Full document details: PD ISO/TS 20459:2023

Documents
Document Sharing Hub

Road vehicles — Injury risk functions for advanced pedestrian legform impactor (aPLI)

1 Scope

This document provides definitions, symbols and injury probability functions (IPFs) for the thigh, leg and knee intended to be used with the advanced pedestrian legform impactor (aPLI), a standardized pedestrian legform impactor with an upper mass for pedestrian subsystem testing of road vehicles. They are applicable to impact tests using the aPLI at 11,1 m/s involving:

— vehicles of category M1, except vehicles with a maximum mass above 2 500 kg and which are derived from N1 category vehicles and where the driver's position, the R-point, is either forward of the front axle or longitudinally rearwards of the front axle transverse centreline by a maximum of 1 100 mm;

— vehicles of category N1, except where the driver's position, the R-point, is either forward of the front axle or longitudinally rearwards of the front axle transverse centreline by maximum of 1 100 mm;

— impacts to the bumper test area defined by References [1] and [2];

— pedestrian subsystem tests involving use of a legform for the purpose of evaluating compliance with vehicle safety standards.

2 Normative references

There are no normative references in this document.

3 Terms and definitions

For the purposes of this document, the following terms and definitions apply.

ISO and IEC maintain terminology databases for use in standardization at the following addresses:

— ISO Online browsing platform: available at https://www.iso.org/obp

— IEC Electropedia: available at https://www.electropedia.org/

3.1
adult
person who is sixteen years old or older

3.2
advanced pedestrian legform impactor
aPLI
modified pedestrian legform impactor which incorporates a mass representing the inertial effect of the upper part of a pedestrian body to enhance biofidelity and *injury assessment capability* (3.10) of conventional pedestrian legforms

3.3
biofidelity
aspect of the *advanced pedestrian legform impactor (aPLI)* (3.2) capability to represent the impact response of human subjects

© ISO 2023 – All rights reserved

Documents
Document Sharing Hub
Full document details: PD ISO/TS 20459:2023

3.4
BLE height
bonnet leading edge height
height of the geometric trace of the upper most points of contact between a straight edge and the front-end of the car

3.5
bumper test area
test area of the legform to bumper impact test

3.6
bumper system
component installed at the hip joint inside the upper mass composed of the bumper, the bumper mount and the compression surface, designed to apply a force on the upper part of the femur in adduction to enhance *injury assessment capability* (3.10) of the *advanced pedestrian legform impactor (aPLI)* (3.2)

3.7
EE method
energy-equivalent method
method of developing *injury probability functions (IPFs)* (3.11) for the *advanced pedestrian legform impactor (aPLI)* (3.2) by transferring human injury values to those of an aPLI using the absorbed energy

3.8
high-bumper car
car with a *lower bumper reference line height* (3.14) of 425 mm or more

3.9
hip joint
uniaxial joint that allows abduction and adduction and connects the upper mass with the lower limb

3.10
injury assessment capability
aspect of the *advanced pedestrian legform impactor (aPLI)* (3.2) capability to produce peak injury values that correlate with those obtained from human body model impact simulations

3.11
IPF
injury probability function
function which defines the relationship between a peak value of an injury metric and probability of injury for a specific load case

3.12
ISO metric
objective rating metric used in this document to verify time histories of sensor output against experimentally or computationally produced target time histories as detailed in ISO/TS 18571:2014

3.13
low-bumper car
car with a *lower bumper reference line height* (3.14) less than 425 mm

3.14
LBRL height
lower bumper reference line height
height of the geometric trace of the lowermost points of contact between a straight edge and the bumper, measured from the ground

3.15
low-pass filter
filter which permits only low-frequency (100 Hz or less) oscillations

© ISO 2023 – All rights reserved
Documents
Document Sharing Hub
Full document details: PD ISO/TS 20459:2023

3.16
paired test method
method of developing *injury probability functions (IPFs)* (3.11) by correlating human injury occurrence in a specific impact configuration with the injury value measured by an ATD subjected to the same impact as detailed in ISO/TR 12350:2013

3.17
subsystem test
test to evaluate safety performance of cars where subsystem impactors representing individual body regions of a pedestrian are propelled into a front end of a stationary car, in impact conditions representing specific load cases in car-pedestrian accidents

3.18
transfer function
TF
linear regression function between human injury values predicted by human body models and *advanced pedestrian legform impactor (aPLI)* (3.2) injury values

3.19
TF method
transfer-function method
method of developing *injury probability functions (IPFs)* (3.11) for the *advanced pedestrian legform impactor (aPLI)* (3.2) by converting human IPFs to those of the aPLI using corresponding *transfer functions* (3.18)

4 Symbols and abbreviated terms

4.1 Symbols

See Table 1.

Table 1 — Symbols and their meanings

Symbol	Meaning
C_{Scale}	Parameter determined for the Weibull distribution for human IPFs
C_{Shape}	Parameter determined for the Weibull distribution for human IPFs
C_{Slope}	Slope of the transfer function
C_{μ}	Parameter determined for the Log-Normal distribution for human IPFs
C_{σ}	Parameter determined for the Log-Normal distribution for human IPFs
C_{TA1}	Correction factor determined to adjust to the real-world accident data
C_{TA2}	Correction factor determined to adjust to the real-world accident data
F	IPF for human
G	Transfer function
I_{human}	Injury metric for human
I_{aPLI}	Injury metric for the aPLI
P	Injury probability of human
P_{adj}	Adjusted injury probability for the MCL
x_{aPLI}	Value of the injury metric for the aPLI
x_{human}	Value of the injury metric for human

© ISO 2023 – All rights reserved

Documents
Document Sharing Hub
Full document details: PD ISO/TS 20459:2023

4.2 Abbreviated terms

See Table 2.

Table 2 — Abbreviated terms and their meanings

Abbreviation	Meaning
ACL	Anterior Cruciate Ligament
aPLI	advanced Pedestrian Legform Impactor
ATD	Anthropometric Test Device
BLE	Bonnet Leading Edge
BM	Bending Moment
BP	Bumper
EE	Energy Equivalent
EEVC	European Enhanced Vehicle-safety Committee
FE	Finite Element
HBM	Human Body Model
IPF	Injury Probability Function
LBRL	Lower Bumper Reference Line
MCL	Medial Collateral Ligament
PCL	Posterior Cruciate Ligament
PMHS	Post Mortem Human Subjects
RCM	Real Car Model
SCM	Simplified Car Model
SP	Spoiler
STP	Subsystem Test Procedure
TF	Transfer Function
TG	Task Group

5 IPFs for the aPLI

5.1 General

The IPFs specified in this document are to be used with the aPLI for the thigh, leg and knee to predict the probability of injuries to pedestrians when involved in real-world car-pedestrian accidents. The IPFs provide a statistically derived relationship between the maximum values of injury metrics obtained from a test conducted using the aPLI by following the subsystem test procedure (STP), and the probability of injury to a corresponding body region of a pedestrian when subjected to load cases representative of the majority of real-world accidents.

The specific load case represented by the subsystem legform test is described below:

— pedestrian size and weight: 175,1 cm and 76,7 kg representing a 50th percentile adult male (Reference [3]);

— impact speed: 11,1 m/s;

— impact direction: lateral-to-medial direction to a pedestrian lower limb;

— lower-limb posture: upright (vertical to the ground) with the knee fully extended;

— impact height: sole of the foot positioned 25 mm above the ground to represent a shoe sole height.

© ISO 2023 – All rights reserved
Documents
Document Sharing Hub
Full document details: PD ISO/TS 20459:2023

First, human IPFs were determined using human biomechanical data available from the literature. Data obtained by the experiments conducted under the loading conditions equivalent to those specified in the STP were referred to. The statistical method used to derive human IPFs follows that recommended by ISO/TS 18506 with the covariates of pedestrian size, weight and age. The pedestrian size and weight were determined from those specified in STP. The age was set at 60 years old that corresponds to the average age of the subjects of the biomechanical data as this choice was found to provide the most reasonable set of assumptions when the IPFs were fitted to the accident data. The recommended method estimates parameters of any one of the Weibull, Log-Normal or Log-Logistic distribution (choose the one that best fits to data) with survival analysis method. In this document, one of the three distributions (Weibull distribution, Log-Normal distribution or Log-Logistic distribution) is used to define human IPFs for each of the injury metrics. The formulae of the aPLI IPFs for these distributions are presented below.

The injury probability when the Weibull distribution is applied following Formula (1):

$$P = 1 - \exp\left\{-\left(\frac{C_{\text{Slope}} \times x_{\text{aPLI}}}{C_{\text{Scale}}}\right)^{C_{\text{Shape}}}\right\} \tag{1}$$

where

P is the injury probability of human;

C_{Scale} is the parameter determined for the Weibull distribution for human IPFs;

C_{Shape} is the parameter determined for the Weibull distribution for human IPFs;

C_{Slope} is the slope of the transfer function (TF);

x_{aPLI} is the value of the injury metric for the aPLI.

The injury probability when the Log-Normal distribution is applied following Formula (2):

$$P = \frac{1}{C_\sigma \sqrt{2\pi}} \int_0^{C_{\text{Slope}} \times x_{\text{aPLI}}} \frac{1}{t} \exp\left\{\frac{-(\ln t - C_\mu)^2}{2C_\sigma{}^2}\right\} \mathrm{d}t \tag{2}$$

where

P is the injury probability of human;

C_μ is the parameter determined for the Log-Normal distribution for human IPFs;

C_σ is the parameter determined for the Log-Normal distribution for human IPFs;

C_{Slope} is the slope of the TF;

x_{aPLI} is the value of the injury metric for the aPLI.

The injury probability when the Log-Logistic distribution is applied following Formula (3):

$$P = \frac{1}{1 + \left(\frac{C_{\text{Slope}} \times x_{\text{aPLI}}}{\exp(C_{\text{Scale}})}\right)^{\frac{-1}{C_{\text{Shape}}}}} \tag{3}$$

where

P is the injury probability of human;

C_{Scale} is the parameter determined for the Log-Logistic distribution for human IPFs;

© ISO 2023 – All rights reserved

AVA Documents Document Sharing Hub
Full document details: PD ISO/TS 20459:2023

C_{Shape} is the parameter determined for the Log-Logistic distribution for human IPFs;

C_{Slope} is the slope of the TF;

x_{aPLI} is the value of the injury metric for the aPLI.

For each of the thigh, leg and knee, IPFs for a human body are then transferred to those of the aPLI using a TF, which is a linear function between the maximum values of a human and aPLI injury metrics. Due to the lack of biomechanical data, the TFs were determined from the results of computational impact simulations using FE human body models (HBMs) and aPLI FE models in loading conditions specified in the STP. Details of the human IPFs from which IPFs for the aPLI are derived can be found in A.2.3. For the determination of TFs, see A.2.4 for more details.

As the IPFs converted from human IPFs using TFs are for the specific load case defined in the STP, the number of injuries calculated from each of the injury probabilities predicted by the IPFs were compared with that of real-world accidents. The IPFs for the knee and the leg were compensated for the real-world observations for the injury metrics showing a significant inconsistency with accident data. Details of the compensation to real-world accidents can be found in Annex B.

Supplemental information related to the TFs and IPFs for human is provided in Annex C and Annex D, respectively.

5.2 Thigh

The IPF for the thigh defines probability of femur shaft fracture to a pedestrian subjected to the load cases representative of the majority of real-world accidents as a function of maximum value of the femur bending moment measured by the aPLI.

Figure 1 presents the IPF for the thigh. The injury probability function is shown in a solid line, with the 95 % confidence interval shown in dotted lines. The horizontal axis represents the maximum value of the femur bending moment measured by the aPLI, and the vertical axis represents the probability of injury.

The IPF for the thigh is given by Formula (4):

$$P = 1 - \exp\left\{-\left(\frac{C_{\text{Slope}} \times x_{\text{aPLI}}}{C_{\text{Scale}}}\right)^{C_{\text{Shape}}}\right\} \tag{4}$$

where

P is the injury probability for the femur shaft of human;

C_{Scale} is the parameter determined for the Weibull distribution for the human IPF for the femur shaft as described in A.2.3.4.1;

C_{Shape} is the parameter determined for the Weibull distribution for the human IPF for the femur shaft as described in A.2.3.4.1;

C_{Slope} is the slope of the TF for the thigh as described in A.2.4.4.1;

x_{aPLI} is the femur BM measured by the aPLI in Nm.

The parameters needed to define the IPF (C_{Scale}, C_{Shape} and C_{Slope}) for the function are described in Table 3.

© ISO 2023 – All rights reserved
Documents
Document Sharing Hub
Full document details: PD ISO/TS 20459:2023

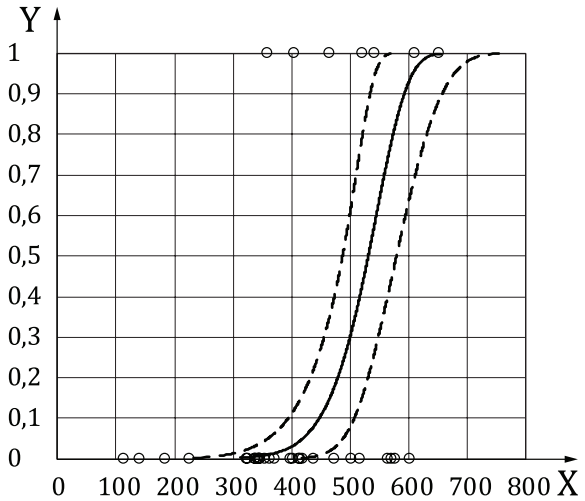

Key

X	aPLI femur BM [Nm]
Y	probability of femur shaft fracture
———	aPLI IPF for femur shaft
= = =	95 % confidence interval
○	observed data

Figure 1 — IPF for the femur shaft

Table 3 — Parameters of IPF for the femur shaft

C_{Scale}	C_{Shape}	C_{Slope}
571	11,0	1,04

5.3 Leg

The IPF for the leg defines probability of tibia shaft fracture to a pedestrian subjected to the specific load cases representative of the majority of real-world accidents as a function of maximum value of the tibia bending moment measured by the aPLI.

Figure 2 presents the IPF for the leg. The injury probability function is shown in a solid line, with the 95 % confidence interval shown in dotted lines. The horizontal axis represents the maximum value of the tibia bending moment measured by the aPLI, and the vertical axis represents the probability of injury.

The IPF for the leg is given by the Formula (5):

$$P = 1 - \exp\left\{-\left(\frac{C_{Slope} \times x_{aPLI}}{C_{Scale}}\right)^{C_{Shape}}\right\} \tag{5}$$

where

P is the injury probability for the tibia shaft of human;

C_{Scale} is the parameter determined for the Weibull distribution for the human IPF for the tibia shaft as described in B.3.3;

© ISO 2023 – All rights reserved

Documents
Document Sharing Hub
Full document details: PD ISO/TS 20459:2023

C_{Shape} is the parameter determined for the Weibull distribution for the human IPF for the tibia shaft as described in B.3.3;

C_{Slope} is the slope of the TF for the leg as described in A.2.4.4.2;

x_{aPLI} is the tibia BM measured by the aPLI in Nm.

The parameters needed to define the IPF (C_{Scale}, C_{Shape} and C_{Slope}) for the function are described in Table 4.

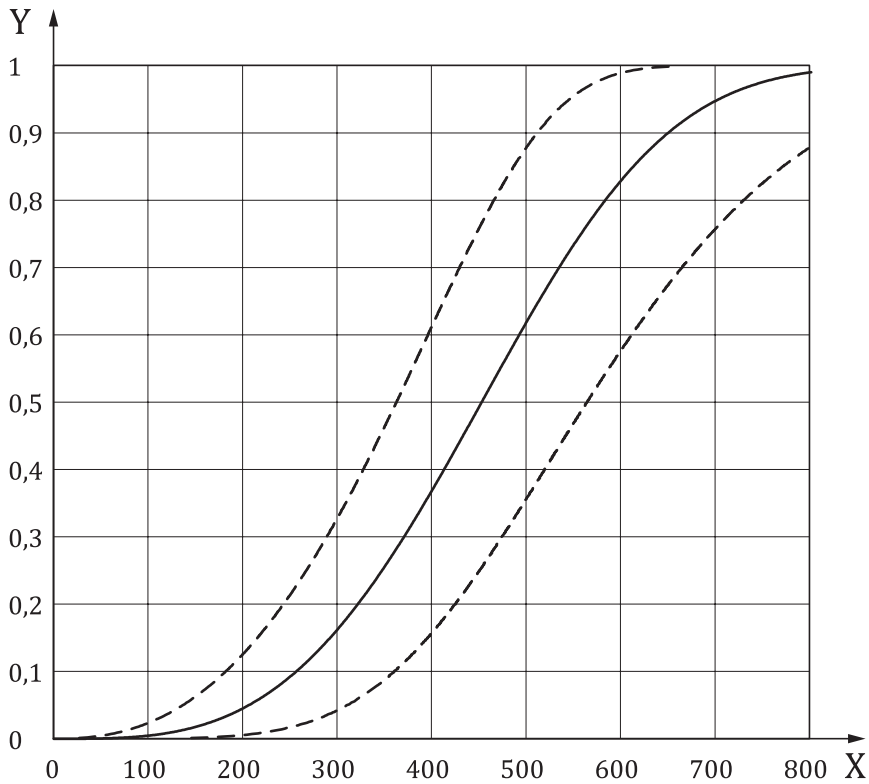

Key

X aPLI tibia BM [Nm]

Y probability of tibia shaft fracture

_____ aPLI IPF for tibia shaft

= = = 95 % confidence interval

Figure 2 — IPF for the tibia shaft

Table 4 — Parameters of IPF for the tibia shaft

C_{Scale}	C_{Shape}	C_{Slope}
446	3,32	0,881

5.4 Knee

The IPF for the knee defines probability of complete failure of the MCL to a pedestrian subjected to the specific load cases representative of the majority of real-world accidents as a function of maximum value of MCL elongation measured by the aPLI.

© ISO 2023 – All rights reserved
Documents
Document Sharing Hub
Full document details: PD ISO/TS 20459:2023

Figure 3 presents the IPF for the knee. The injury probability function is shown in a solid line, with the 95 % confidence interval shown in dotted lines. The horizontal axis represents the maximum value of the MCL elongation measured by the aPLI, and the vertical axis represents the probability of injury.

The IPF for the knee is given by Formula (6):

$$P = \frac{1}{C_\sigma \sqrt{2\pi}} \int_0^{C_{\text{Slope}} \times x_{\text{aPLI}} \times C_{\text{TA1}} \times C_{\text{TA2}}} \frac{1}{t} \exp\left\{ \frac{-\left(\ln t - C_\mu\right)^2}{2 C_\sigma{}^2} \right\} \mathrm{d}t \tag{6}$$

where

P is the injury probability for the MCL of human;

C_μ is the parameter determined for the Log-Normal distribution for human IPFs for the MCL as described in A.2.3.4.3;

C_σ is the parameter determined for the Log-Normal distribution for human IPFs for the MCL as described in A.2.3.4.3;

C_{Slope} is the slope of the TF for the knee as described in A.2.4.4.3;

C_{TA1} is the correction factor for lower-limb posture and impact angle determined to adjust to the real-world accident data as described in B.3.2.2.4;

C_{TA2} is the correction factor for muscle tone determined to adjust to the real-world accident data as described in B.3.2.3;

x_{aPLI} is the MCL elongation measured by the aPLI in mm.

The parameters needed to define the IPF (C_μ, C_σ, C_{Slope}, C_{TA1} and C_{TA2}) for the function are described in Table 5.

© ISO 2023 – All rights reserved

Documents
Document Sharing Hub
Full document details: PD ISO/TS 20459:2023

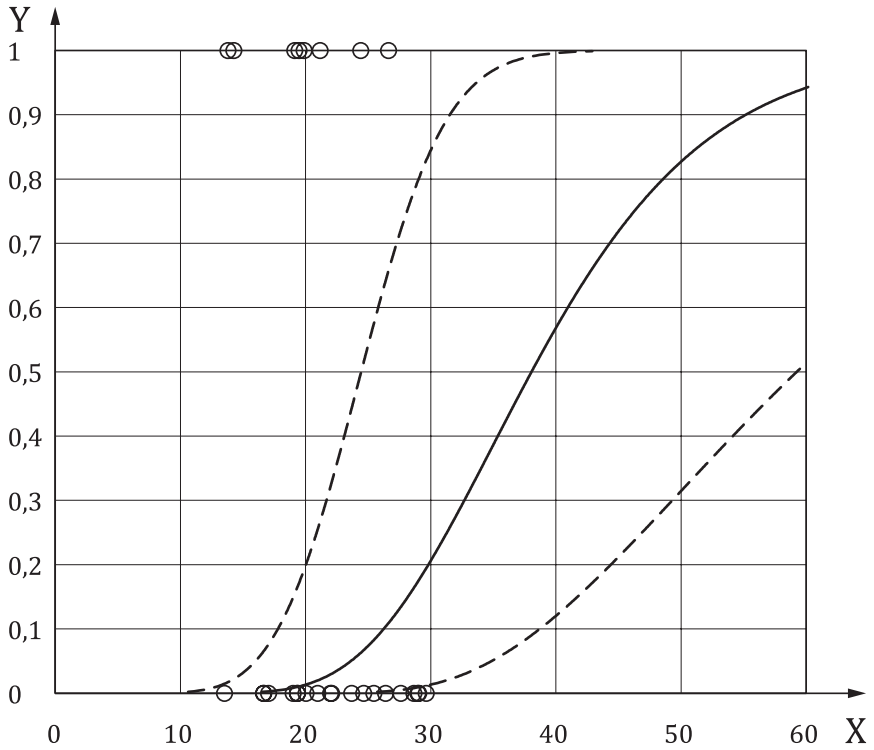

Key

X	aPLI MCL elongation [mm]
Y	probability of MCL complete rupture
———	aPLI IPF for MCL complete rupture
= = =	95 % confidence interval
○	observed data

Figure 3 — IPF for the MCL complete rupture

Table 5 — Parameters of IPF for the MCL complete rupture

C_{μ}	C_{σ}	C_{Slope}	C_{TA1}	C_{TA2}
3,34	0,291	1,14	0,72	0,90

© ISO 2023 – All rights reserved
Documents
Document Sharing Hub
Full document details: PD ISO/TS 20459:2023

Annex A
(informative)

Rationale regarding background and methodology to develop IPFs for the aPLI

A.1 Historical background

A.1.1 General

Although lower extremity injuries are not life-threatening, they are frequent and potentially disabling, resulting in a substantial cost to the victims and society. The importance of preventing this type of injuries is illustrated by the United Nation (UN) regulations that aim to mitigate lower extremity injuries to pedestrians hit by the front-end of cars (See References [1] and [2]).

The UN regulations initially implemented the EEVC pedestrian legform impactor that simply consists of rigid long bones and a deformable knee joint. In order to improve injury assessment capability, a new impactor called the Flexible Pedestrian Legform Impactor (FlexPLI) has been developed and implemented in the phase-2 of Reference [1].

Despite a number of improvements of its capability relative to the EEVC impactor, the FlexPLI still lacks representation of the influence of the upper part of the body. To address technical issues with the FlexPLI, including but not limited to the lack of upper body representation, the aPLI with the upper mass attached to the top of the conventional pedestrian legform to compensate for the lack of the upper body has been developed. In November 2014, two ISO projects were initiated to develop Technical Specification (TSs) for "Road vehicles - Modified pedestrian legform impactor for tests of high bumper vehicles" and "Road vehicles - Injury criteria and risk curves for a modified pedestrian legform impactor for use with high bumper vehicles", and the aPLI task group (TG) was established by active participants from research institutes, dummy and instruments manufacturers, governments and car manufacturers. The aPLI TG has conducted extensive CAE studies to identify optimized specifications of the aPLI by utilizing HBMs, SCMs and aPLI prototype models. Based on the specifications identified, a physical version of aPLI SBL-A was fabricated and subjected to international round robin testing.

The aPLI TG also dedicated to their effort to discuss a methodology to develop IPFs. During the discussion, two different methods were proposed and it was difficult to choose one of the two proposed methods because both have pros and cons. A new idea taken to facilitate the discussion was to develop ‘virtual IPFs’ by using parametric human body models (HBMs) with the variability in the material property of a human body incorporated. The results of this analysis along with some other consideration resulted in a decision of applying a TF to convert IPFs for human to those for the aPLI.

Due to the lack of sufficient biomechanical data, it was necessary to determine TFs based on the results of computer simulations using HBMs to take various load cases into consideration. Multiple HBMs with extensive validation were used to avoid potential bias in case one single HBM is employed. The specifications of the latest version of the aPLI hardware with the bumper system installed at the hip joint as defined in ISO/TS 20458 were represented by FE models and used in the analyses. Real car models (RCMs) were also used to accurately represent geometric and stiffness characteristics of car front-end structures. The use of multiple different HBMs, RCMs and impact locations allowed determination of robust IPFs.

In the course of the discussion at the aPLI TG, a question was raised as to real-world relevance of the IPFs determined in this international effort. The most important decision made by the aPLI TG was that IPFs shall predict the probability of injury to a pedestrian involved in a real car accident, not necessarily to a pedestrian hit by a car in a load case specified in the STP. This approach would require adjustment of IPFs to match field observations, if the load case specified by the STP does not represent real-world

© ISO 2023 – All rights reserved

AVA Documents Document Sharing Hub
Full document details: PD ISO/TS 20459:2023

accidents. Among the three body regions (thigh, knee and leg) for which injury values are measured by the aPLI, a preliminary study done by the aPLI TG revealed that a significant discrepancy in the prediction of the probability of injury is seen specifically with the MCL elongation, due to the upright lower limb position and fully extended knee specified in the STP, and the lack of consideration of the influence of muscle tone. For this reason, the aPLI TG decided to adjust aPLI IPFs to match real-world observations in such a way that injury metrics obtained from an aPLI car test are converted to the probability of injury in real-world accidents.

IPFs for human that represent the load case specified in the STP were initially developed because the biomechanical data available in the literature are from experimental studies that used boundary conditions representing this load case. By applying the TFs, the IPFs for humans were transformed to the IPFs for the aPLI that predict the probability of injury in the load case specified in the STP. The number of injuries estimated from the probability of injury predicted by these IPFs was compared to that of the real-world accidents for each of the injury metrics for the aPLI. Whenever a significant inconsistency with the field observation was identified, factors responsible for the discrepancy were investigated using literature review, HBMs and multiple car models. Based on the results of the investigation, the IPFs for the knee and leg were adjusted to the real-world accident data as described in Annex B. The adjusted IPFs were further modified to better match the field observations as needed.

A.1.2 Need for standardized IPFs for the aPLI

Due to the lack of the upper body, the legform test in the pedestrian STP allows assessment of knee and leg regions only, necessitating a different test procedure for the thigh region with a different impactor and a test protocol. The lack of biofidelity of the upper legform requires a modified legform with upper body representation. In addition, a large approach angle of a high-bumper car results in significantly different kinematics of a legform, leading to a need for a different test procedure specifically defined for such cars and inconsistency of the bumper test.

For these reasons, new car assessment programs have been interested in introducing a modified legform test capable of replacing the upper legform tests and enhancing injury assessment. In order to avoid unreasonable increase of the cost to car manufacturer, and therefore to customers, of developing different car structures and/or protection systems to comply with different requirements, a globally accepted and harmonized test tool is crucial for future upgrade of a test procedure for consumer information and regulatory testing. Accurate prediction of injury probability in real-world accidents from the test results using such an advanced test tool is also vital to take the best advantage of the tool.

A.1.3 Benefits and economic impact of standardized IPFs for the aPLI

Robustness of IPFs is crucial to determine injury assessment reference values (IARVs) suitable for globally harmonized use. When investigating correlation between human and aPLI impact responses to develop IPFs based on biomechanical data, this requires consideration of various shapes and stiffness distributions of front-ends of cars, along with multiple different HBMs that have been well validated against biomechanical data. An international effort provided by the experts of the aPLI TG has allowed incorporation of various impact configurations from a variety of combinations of cars in different markets and HBMs.

With regard to the benefits, globally harmonized and scientifically valid IPFs for the aPLI are essential to determine reasonable IARVs for future regulations and/or new car assessment programs. It is also crucial that the IPFs predict the probability of injury in a load case representative of real-world accidents, not necessarily the load case specified in a test procedure in case it is not representative. Determination of reasonable IARVs would ensure effectiveness of pedestrian safety measures of cars in real-world accidents, and eliminate potentially wasteful and misleading efforts of car manufacturers needed to develop cars to comply with the requirements imposed by unreasonable IARVs. This also reduces costs to consumers, along with the reduction of social costs due to injuries to pedestrian lower limbs.

© ISO 2023 – All rights reserved
Documents
Document Sharing Hub
Full document details: PD ISO/TS 20459:2023

A.1.4 Survey and general differences from previous IPFs

The IARVs for the FlexPLI have been determined for References [1] and [2] by the informal group on UN GTR No.9 Phase-2 under the UN working party on passive safety (GRSP). Due to the lack of globally accepted IPFs for the FlexPLI, the discussion to determine IARVs has been a big challenge, involving proposals from different rationale and concepts. In such a situation, both technical and political discussions were mixed up, making it difficult to clarify benefits in a consistent manner. This has led to a strong need for a globally accepted and scientifically valid IPFs for the aPLI, which is anticipated to be used in future regulatory and consumer information testing.

In the course of the discussion on the FlexPLI IARVs, IPFs for the FlexPLI have been developed using biomechanical data[6]. Although a similar methodology to that used to develop IPFs for the aPLI was used, there are some limitations due to the statistical method used and limited robustness of the TFs. A combination of geometric scaling of injury values and a univariate survival model was applied for the FlexPLI, while a multivariate survival model used for the aPLI defined injury probability as a function of the height, the weight and the age of a pedestrian to enhance accuracy of prediction models. When developing TFs for the FlexPLI, impact simulations were conducted using one single HBM and simplified car models (SCMs) representing geometric and stiffness characteristics of old sedans at one single impact location. The robustness of TFs for the aPLI has been significantly enhanced by using multiple HBMs and RCMs representing various types of cars in a global fleet, along with impact simulations at multiple impact locations. In addition, the relevance of the IPFs for FlexPLI were not validated against accident data, while the IPFs for the aPLI were adjusted to real-world observations whenever needed. The enhancement in the statistical method and the robustness of TFs, along with the adjustment of the IPFs to real-world accident data, would lead to more accurate prediction of the probability of injury to a pedestrian lower limb when involved in a car-pedestrian accident, and consequently contribute to further improvement in pedestrian safety performance of cars in a global market.

A.1.5 Summary of development process of IPFs for the aPLI

The following summarizes some of the milestones in the aPLI project, in order to describe the international development and consensus process.

— June 2015: The aPLI TG was established by ISO TC 22/SC 36/WG 5 and WG 6.

— November 2017: At the 6th aPLI TG meeting, it was recognized by aPLI TG members that the paired test method (ISO/TR 12350:2013)[4] is not applicable to develop IPFs for the aPLI because of the lack of sufficient biomechanical data, and two alternatives, the TF method and the EE method as detailed in Annex A.2.2.2.2 and Annex A.2.2.2.3, respectively, were proposed by some of aPLI TG members.

— May 2018: The idea of a virtual paired test was proposed by some of aPLI TG members at the 7th aPLI TG meeting to evaluate the two methods to develop IPFs for the aPLI.

— June 2019: The aPLI TG decided at its 9th meeting in London to use the TF method based on the results of the virtual paired test and the comparison of the number of biomechanical data available for each of the two methods.

— June to December 2020: Due to the pandemic situation of COVID-19, aPLI TG activity was put on hold, and official discussions on the development of IPFs for human and TFs have been suspended.

— February 2021: The aPLI TG activity was restarted and it was endorsed to adjust the IPFs to real-world accident data. A draft version of ISO/TS 20459 was submitted to the aPLI TG for review.

— March to August 2021: Due to continued pandemic of COVID-19, aPLI TG activity was put on hold again.

— August 2021: The aPLI TG activity was officially restarted.

— March 2022: A modified draft version of ISO/TS 20459 incorporating the IPFs for the aPLI was accepted by the aPLI TG and submitted to ISO TC22/SC36/WG6 for their review.

© ISO 2023 – All rights reserved

Documents
Document Sharing Hub
Full document details: PD ISO/TS 20459:2023

— May 2022: The draft version of ISO/TS 20459 was further modified based on the comments from WG6 and was approved by WG6. The document was immediately subjected to a ballot of ISO TC22/SC36.

— July 2022: The proposed ISO/TS 20459 was approved by ISO TC22/SC36 with some requests for modification.

Organizationally, at every stage, the aPLI TG attempted to include all interested parties involved in the pedestrian safety field worldwide. In particular, 28 aPLI TG web meetings were held in between face-to-face meetings to facilitate discussions and consensus development by all participants. All the development activities were conducted at the expense of participating parties. Collaborative CAE studies to develop TFs were conducted by contributors from Germany, France, the United States and Japan.

A.2 Methodology to develop IPFs for the aPLI

A.2.1 General

Any assessment of car safety performance shall provide information relevant to the probability of injury sustained by the victims involved in real-world car accidents, not in laboratory car crash tests. In general, testing and assessment protocols are designed to provide such information. In the case of the assessment of safety performance against pedestrian lower limb injury, the aPLI TG recognized a large discrepancy between the two load cases, specifically with the MCL elongation. Once IPFs for the aPLI consistent with the STP are developed, the relevance of the IPFs against accident data shall be evaluated. The IPFs shall be adjusted to represent injury probability in real-world accidents when inconsistency is found to be significant.

IPFs for the aPLI were developed by the following steps. First, human biomechanical data were collected to develop IPFs for the aPLI. The results of the experiments performed under the conditions similar to the load case specified in the STP were used. The conditions included regions of the lower limb, specific injuries reproduced, relevant injury metrics to predict such injuries, and specific load cases such as the loading rate, loading direction and lower-limb posture. Second, a methodology to develop IPFs for the aPLI in a load case specified in the STP was determined. This step was one of the most challenging one among all the steps employed. Due to the lack of sufficient biomechanical data available, it was impossible to use the method defined by ISO for the WorldSID dummy (paired test method described in ISO/TR 12350), and an alternative method needed to be defined. As a result of intensive discussion by aPLI TG members, it was eventually decided to use the TF method. Third, IPFs for the aPLI were developed by using the TF method. In the TF method, IPFs for human are initially developed, and then converted to those of the aPLI in the load case specified by the STP by applying TFs obtained from a regression analysis of maximum values of injury metrics between aPLI and human. Finally, the relevance of the IPFs was assessed against accident data and the IPFs were adjusted to better represent real-world accident data whenever needed.

More details with regard to the methodology to develop IPFs for the aPLI can be found in the following sections.

A.2.2 Determination of methodology to develop IPFs for the aPLI in a load case specified in the STP as functions of aPLI injury metrics

A.2.2.1 General

The paired test method used by ISO to derive IPFs for WorldSID (ISO/TR 12350) relates injury occurrence to human bodies to injury values from the dummy by performing paired (human and dummy) tests in the same impact configuration. In case of a pedestrian, however, full-scale impact test data using human subjects are scarce, and therefore an alternative methodology to develop IPFs for the aPLI needed to be determined. This resulted in proposals of two alternative methods at the aPLI TG (TF method and EE method), and an extensive study was conducted to make a final decision. As both methods involve pros and cons, a new idea of investigating virtual IPFs was proposed that virtually

© ISO 2023 – All rights reserved
AVA Documents Document Sharing Hub
Full document details: PD ISO/TS 20459:2023

generates biomechanical data using parametric HBMs that incorporate variability of material property of human tissues to allow comparison of IPFs from the two proposed methods against those determined by the paired test method. The results of this investigation along with the difference of the number of data that can be used in each of the two proposed methods resulted in the choice of the TF method at the aPLI TG.

A.2.2.2 Virtual IPF

A.2.2.2.1 Parametric HBM

Due to the lack of a sufficient number of full-scale pedestrian impact test data, full-scale impact test data using human subjects were virtually generated by incorporating variability of the material property of human tissues in a validated HBM (References [7], [8] and [9]) to create parametric HBMs with different material property. Since the material property of human tissue is generally characterized by a constitutive equation that describes the relationship between the stress and the strain, three levels (mean, upper and lower limits) were set for each, resulting in a total of nine parametric HBMs. Assuming that the major contributors to the lower limb injury metrics (femur and tibia bending moment (BM), MCL elongation) are the material property of the cortical bones of the femur, tibia and fibula, along with that of the four major knee ligaments (anterior cruciate ligament (ACL), posterior cruciate ligament (PCL), lateral collateral ligament (LCL) and MCL) and the knee joint capsule, the same material property was used for the flesh, skin and other bones and ligaments for all of the nine HBMs.

The nine parametric HBMs were determined by means of the following procedure. Initially, biomechanical data were investigated for each of the varied material parameters. Assuming that the material property is the same between the tibia and the fibula, and among the four knee ligaments, the following values were obtained from the literature for the cortical bones of the femur and the tibia as well as the four knee ligaments:

a) Young's modulus, ultimate stress and ultimate strain:

— femur: mean and 90 % confidence interval[10];

— tibia: mean and 90 % confidence interval[10];

— knee ligament: mean[10];

b) Ratio of yield stress to ultimate stress:

— tibia[11];

— knee ligament: mean[10].

Using the values of the material parameters obtained above, nine stress-strain curves were determined by means of the following steps. First, for all the material parameters of the femur, the tibia and the fibula, except the yield stress, the mean and the upper and lower limits were determined from the mean and 90 % confidence interval obtained from the literature listed above. As a 90 % confidence interval was not available from the literature for the knee ligaments, a 90 % confidence interval normalized by mean obtained for the femur was applied to each of the Young's modulus, ultimate stress and ultimate strain to estimate the 90 % confidence interval of the corresponding material parameter. Second, nine failure points were determined from the mean and the upper and lower limbs of the ultimate stress and the ultimate strain. Since the data for the ultimate stress and the ultimate strain show bell-shaped distribution, it was assumed that the combinations of the maximum and the minimum values of the ultimate stress/strain are unrealistic. By eliminating these extreme combinations, the nine failure points were distributed on a diamond shape and its centroid, with the mean and the upper and lower limits of the ultimate stress/strain represented by its diagonal lines as shown in Figures A.1 through A.3. Third, the nine failure points were assigned to each of the mean and the upper and lower limits of the Young's modulus determined above. Reference [11] shows that a large Young's modulus for the tibia is associated with a large ultimate stress and a small ultimate strain due to trade-off between brittleness and ductility. This nature was assumed to apply to other tissues as well. For this reason, the nine failure points were grouped into three, each containing three points, in such a way that the

© ISO 2023 – All rights reserved

AVA Documents Document Sharing Hub
Full document details: PD ISO/TS 20459:2023

corresponding points from the three groups are aligned in a downward slope (groups of black, white and grey squares: see Figures A.1 through A.3). Each of the three groups of the three failure points was assigned to each of the three values of the Young's modulus by following the trend described above. Finally, the slope of the plastic region in the stress-strain curve was determined for each of the nine failure points. References [11] and [10] show that the ratio of the yield stress to the ultimate stress is constant for the cortical bone of the tibia as well as the knee ligaments (tibia: 0,82, knee ligaments: 0,82). The same ratio as that of the tibia was applied to the femur due to the lack of available information. In Reference [12] it is found that the stiffness of the toe region, up to 5 % strain, of the stress-strain curve of the knee ligaments is approximately half of that of the subsequent elastic region. This finding was reflected in the stress-strain curves determined for the knee ligaments (see Figure A.3).

The thigh, the leg and the knee of the nine parametric HBMs sufficiently represented the variability of the PMHS responses in a 3-point bending test of the thigh [13][14] and the leg [13][15][14], and 4-point bending test for the knee[16], as shown in Figure A.4 through Figure A.6, respectively. Biomechanical data needed for the TF method, EE method and paired test method were virtually generated using these HBMs, and each of the three methods was applied to calculate IPFs for the thigh, leg and knee.

© ISO 2023 – All rights reserved
Documents
Document Sharing Hub
Full document details: PD ISO/TS 20459:2023

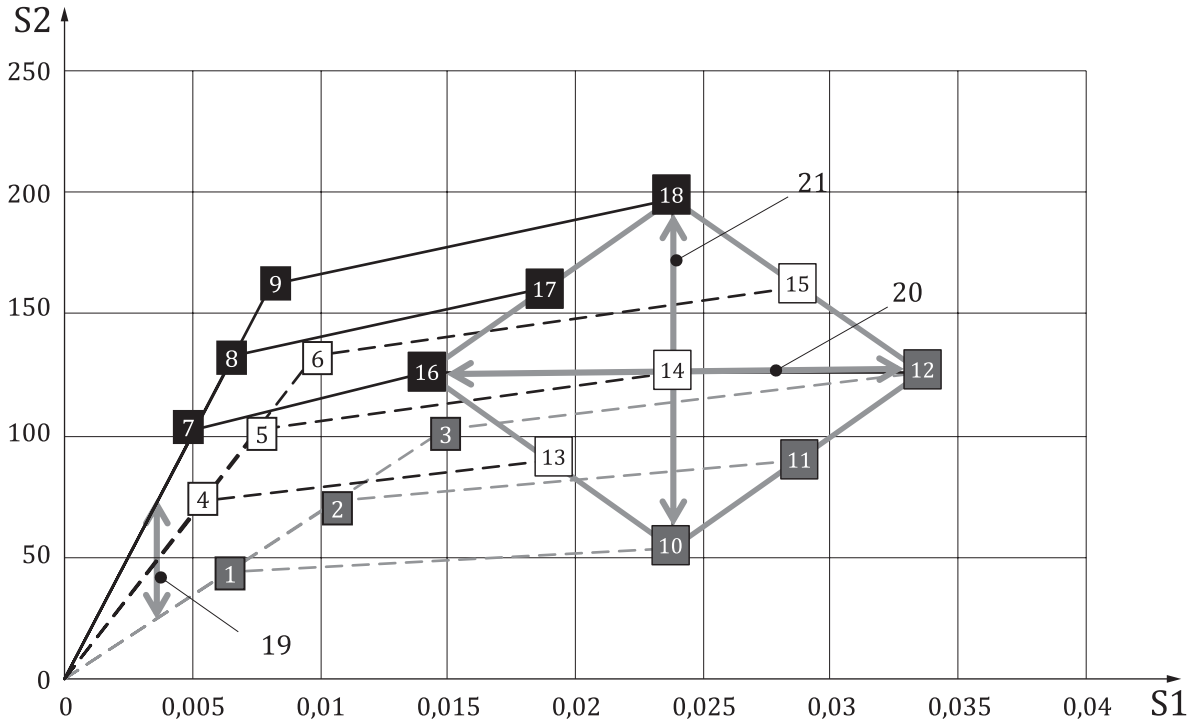

Key

1 yield stress/strain for HBM1
2 yield stress/strain for HBM2
3 yield stress/strain for HBM3
4 yield stress/strain for HBM4
5 yield stress/strain for HBM5
6 yield stress/strain for HBM6
7 yield stress/strain for HBM7
8 yield stress/strain for HBM8
9 yield stress/strain for HBM9
10 ultimate stress/strain for HBM1
11 ultimate stress/strain for HBM2
12 ultimate stress/strain for HBM3
13 ultimate stress/strain for HBM4
14 ultimate stress/strain for HBM5
15 ultimate stress/strain for HBM6
16 ultimate stress/strain for HBM7
17 ultimate stress/strain for HBM8
18 ultimate stress/strain for HBM9
19 90 % confidence interval (young's modulus)
20 90 % confidence interval (ultimate strain)
21 90 % confidence interval (ultimate stress)
S1 strain
S2 stress [MPa]

Figure A.1 — Stress-strain curves of the cortical bone of the femur for the nine parametric HBMs

© ISO 2023 – All rights reserved

Documents
Document Sharing Hub
Full document details: PD ISO/TS 20459:2023

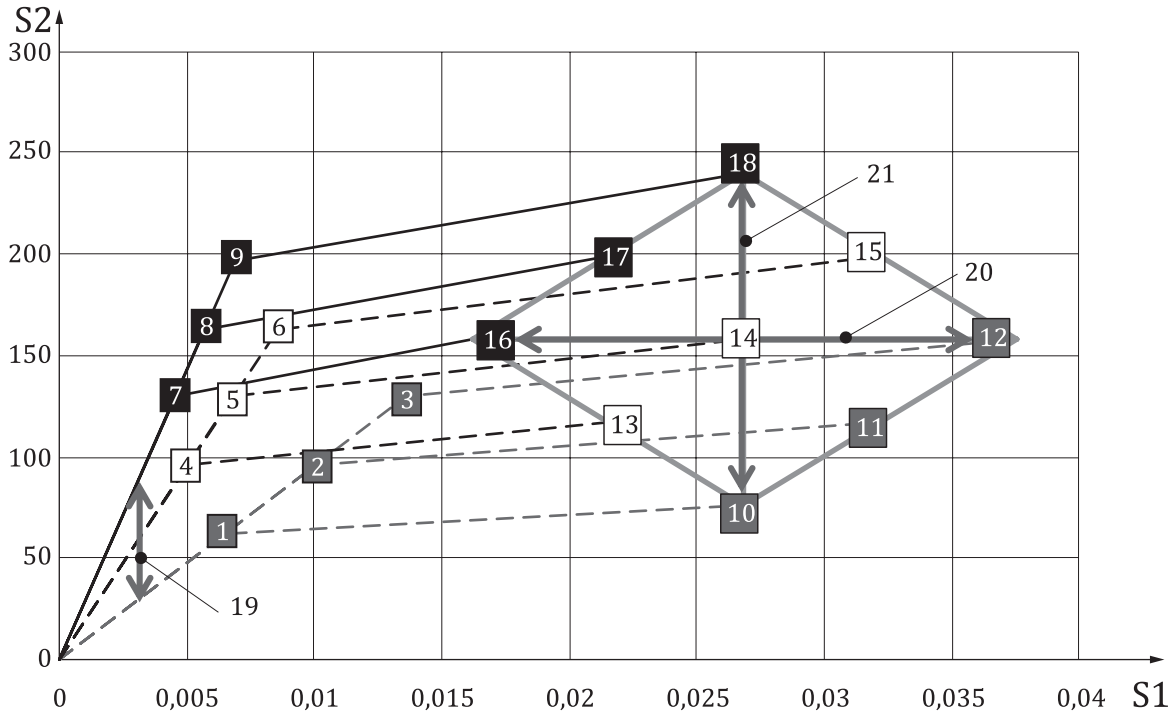

Key

1 yield stress/strain for HBM1
2 yield stress/strain for HBM2
3 yield stress/strain for HBM3
4 yield stress/strain for HBM4
5 yield stress/strain for HBM5
6 yield stress/strain for HBM6
7 yield stress/strain for HBM7
8 yield stress/strain for HBM8
9 yield stress/strain for HBM9
10 ultimate stress/strain for HBM1
11 ultimate stress/strain for HBM2
12 ultimate stress/strain for HBM3
13 ultimate stress/strain for HBM4
14 ultimate stress/strain for HBM5
15 ultimate stress/strain for HBM6
16 ultimate stress/strain for HBM7
17 ultimate stress/strain for HBM8
18 ultimate stress/strain for HBM9
19 90 % confidence interval (young's modulus)
20 90 % confidence interval (ultimate strain)
21 90 % confidence interval (ultimate stress)
S1 strain
S2 stress [MPa]

Figure A.2 — Stress-strain curves of the cortical bone of the tibia for the nine parametric HBMs

© ISO 2023 – All rights reserved
Documents
Document Sharing Hub
Full document details: PD ISO/TS 20459:2023

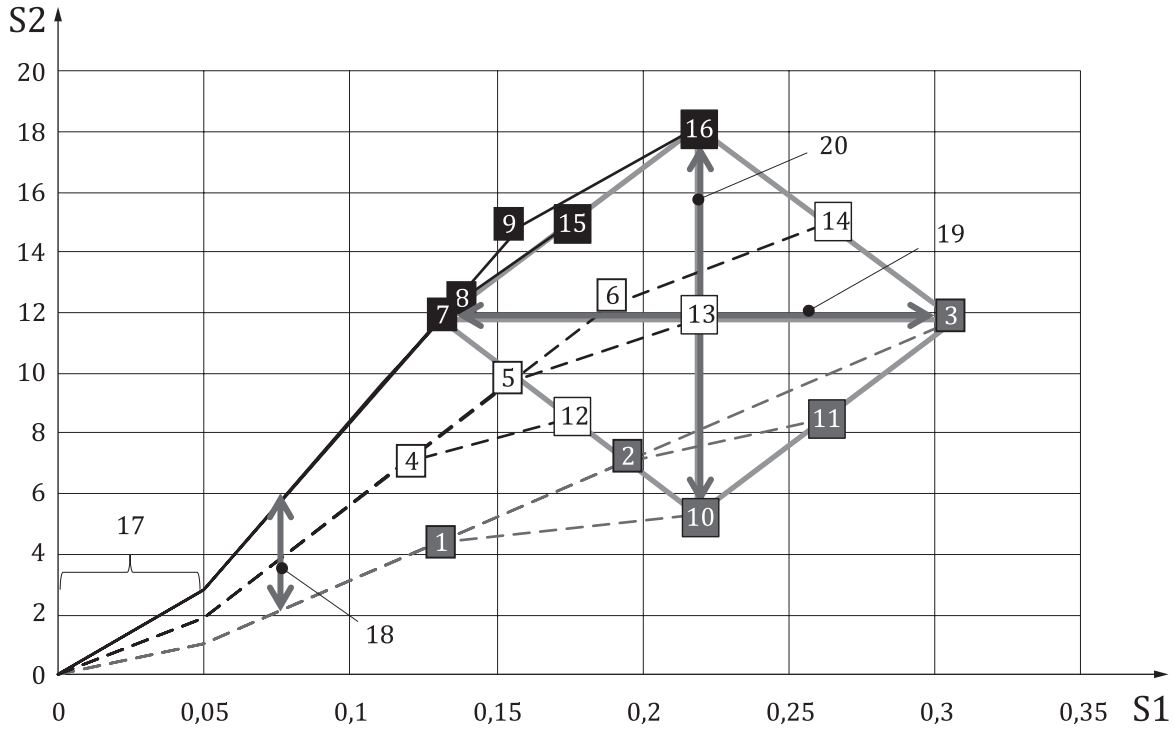

Key

1 yield stress/strain for HBM1
2 yield stress/strain for HBM2
3 yield/ultimate stress/strain for HBM3
4 yield stress/strain for HBM4
5 yield stress/strain for HBM5
6 yield stress/strain for HBM6
7 yield/ultimate stress/strain for HBM7
8 yield stress/strain for HBM8
9 yield stress/strain for HBM9
10 ultimate stress/strain for HBM1
11 ultimate stress/strain for HBM2
12 ultimate stress/strain for HBM4
13 ultimate stress/strain for HBM5
14 ultimate stress/strain for HBM6
15 ultimate stress/strain for HBM8
16 ultimate stress/strain for HBM9
17 half of young's modules region
18 90 % confidence interval (young's modulus)
19 90 % confidence interval (ultimate strain)
20 90 % confidence interval (ultimate stress)
S1 strain
S2 stress [MPa]

Figure A.3 — Stress-strain curves of the knee ligaments for the nine parametric HBMs

© ISO 2023 – All rights reserved

Documents
Document Sharing Hub
Full document details: PD ISO/TS 20459:2023

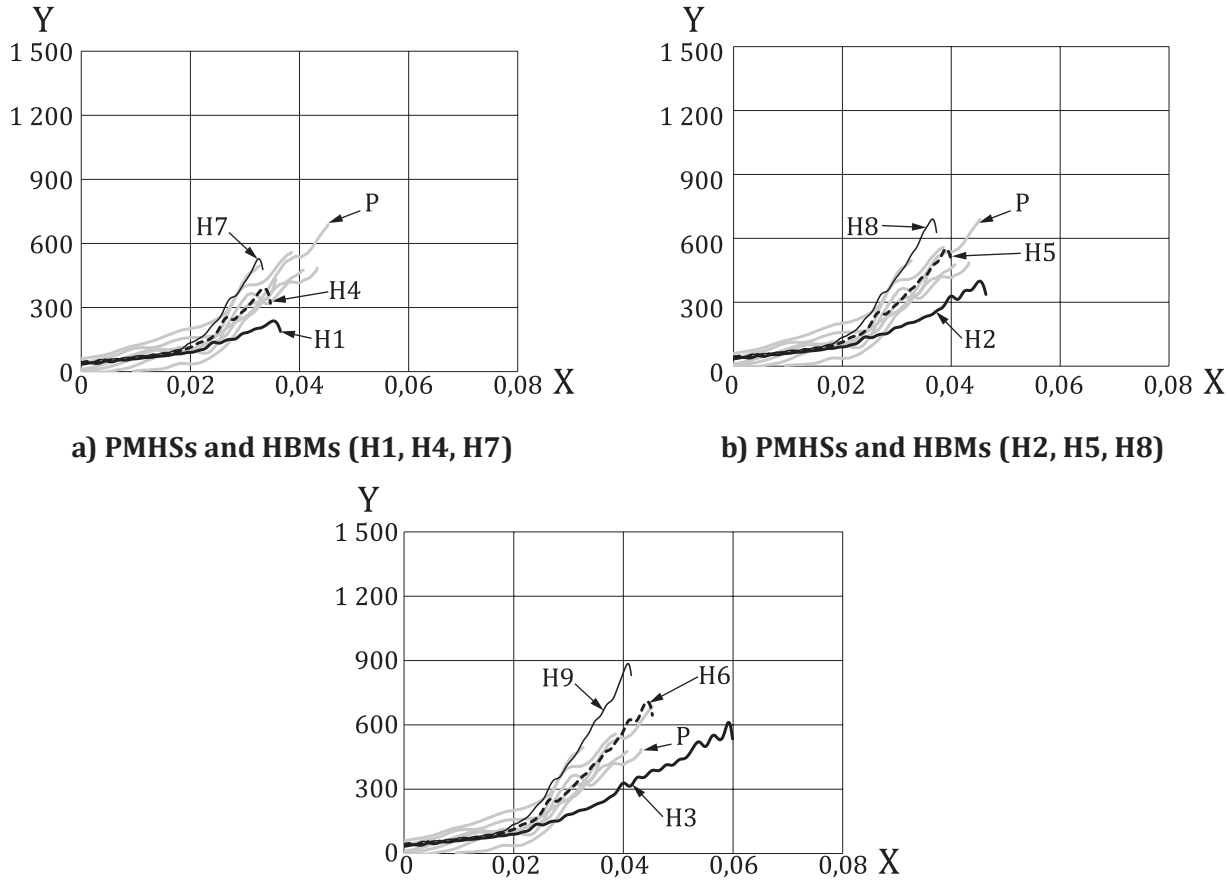

a) PMHSs and HBMs (H1, H4, H7)

b) PMHSs and HBMs (H2, H5, H8)

c) PMHSs and HBMs (H3, H6, H9)

Key

X deflection [m]
Y BM [Nm]
P PMHS test data
H1 computer simulation result of HBM-1
H2 computer simulation result of HBM-2
H3 computer simulation result of HBM-3
H4 computer simulation result of HBM-4
H5 computer simulation result of HBM-5
H6 computer simulation result of HBM-6
H7 computer simulation result of HBM-7
H8 computer simulation result of HBM-8
H9 computer simulation result of HBM-9

Figure A.4 — Comparison of BM-displacement curves for 3-point bending of the thigh between the nine parametric HBMs and PMHSs

© ISO 2023 – All rights reserved
Documents
Document Sharing Hub
Full document details: PD ISO/TS 20459:2023

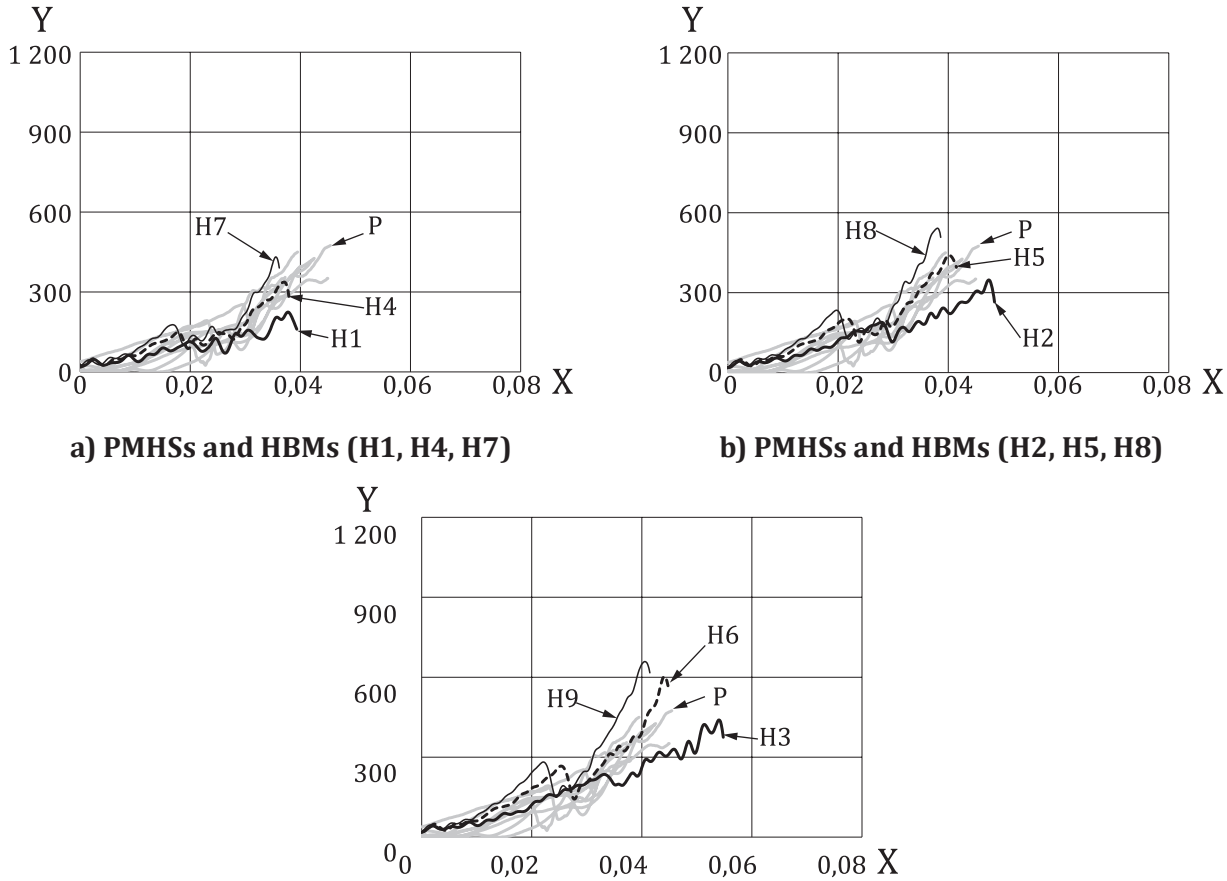

a) PMHSs and HBMs (H1, H4, H7)

b) PMHSs and HBMs (H2, H5, H8)

c) PMHSs and HBMs (H3, H6, H9)

Key

X deflection [m]
Y BM [Nm]
P PMHS test data
H1 computer simulation result of HBM-1
H2 computer simulation result of HBM-2
H3 computer simulation result of HBM-3
H4 computer simulation result of HBM-4
H5 computer simulation result of HBM-5
H6 computer simulation result of HBM-6
H7 computer simulation result of HBM-7
H8 computer simulation result of HBM-8
H9 computer simulation result of HBM-9

Figure A.5 — Comparison of BM-displacement curves for 3-point bending of the leg between the nine parametric HBMs and PMHSs

© ISO 2023 – All rights reserved

Documents
Document Sharing Hub
Full document details: PD ISO/TS 20459:2023

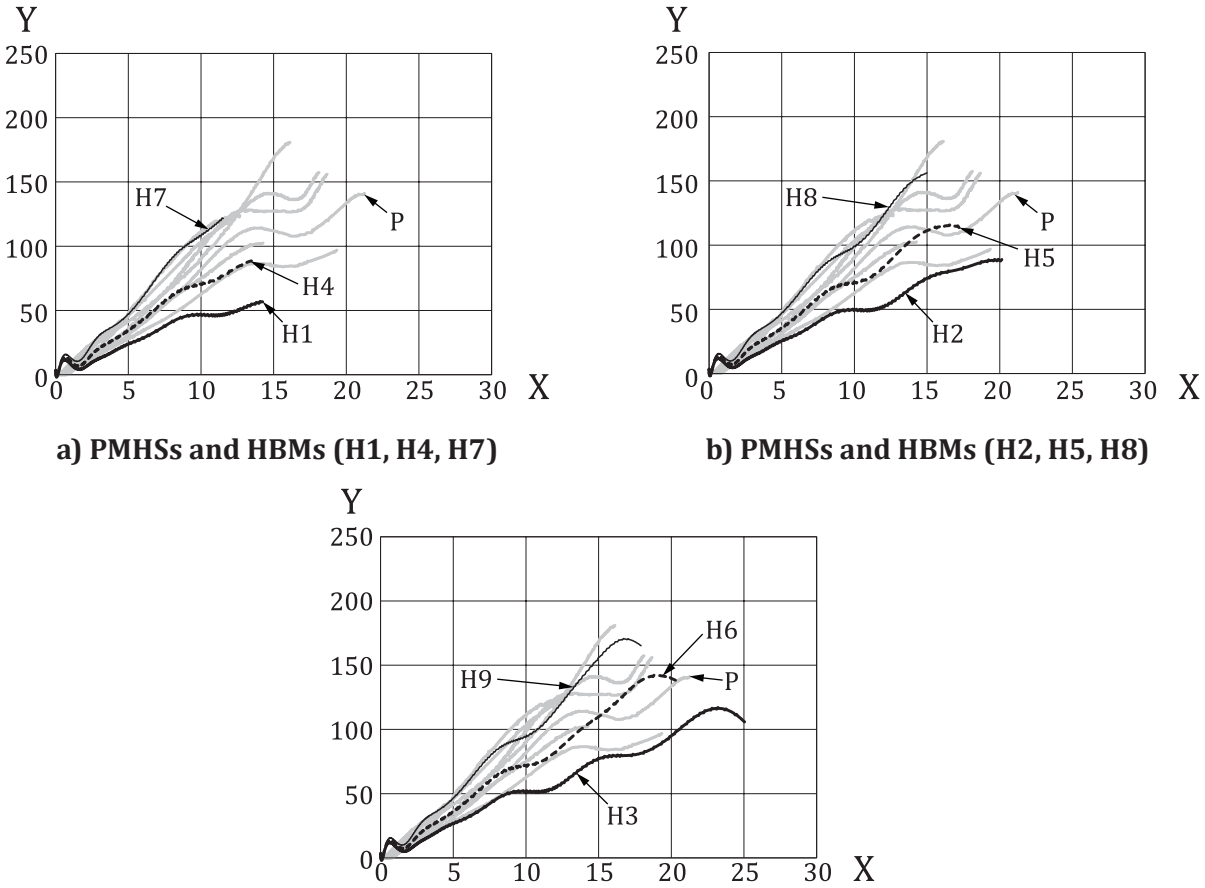

a) PMHSs and HBMs (H1, H4, H7)

b) PMHSs and HBMs (H2, H5, H8)

c) PMHSs and HBMs (H3, H6, H9)

Key

X knee valgus angle [°]

Y BM [Nm]

P PMHS test data

H1 computer simulation result of HBM-1

H2 computer simulation result of HBM-2

H3 computer simulation result of HBM-3

H4 computer simulation result of HBM-4

H5 computer simulation result of HBM-5

H6 computer simulation result of HBM-6

H7 computer simulation result of HBM-7

H8 computer simulation result of HBM-8

H9 computer simulation result of HBM-9

Figure A.6 — Comparison of BM-knee valgus angle curves for 4-point bending of the knee between the nine parametric HBMs and PMHSs

A.2.2.2.2 Transfer-function (TF) method

Due to the lack of sufficient full-scale pedestrian impact test data using human subjects, the TF method initially develops an IPF for humans based on biomechanical data using isolated lower limb segments, such as the thigh, the leg and the knee. Therefore, the IPF for humans represents failure tolerance of each individual lower limb segment. Next, a TF is determined for each lower limb segment by calculating a regression function between the maximum values of the corresponding injury metric for human

© ISO 2023 – All rights reserved

Documents
Document Sharing Hub
Full document details: PD ISO/TS 20459:2023

and the aPLI, when subjected to the same impacts. Impacts are delivered to a full-body pedestrian along with the full assembly of the aPLI to determine the function in a full-scale impact configuration to accurately represent the regression function under the load case specified in the STP. The lack of sufficient full-scale pedestrian impact test data requires the use of HBMs as opposed to actual human subjects. Since the use of computational modelling would make it possible to incorporate a number of different impact conditions with different types of cars at an affordable cost, injury values for the aPLI are also obtained from its computational model. IPFs for the aPLI are then developed by converting human IPFs to those of the aPLI using corresponding TFs. Figure A.7 shows a flow to develop IPFs for the aPLI using the TF method.

First, virtual IPFs for human were developed by applying the TF method to the virtual biomechanical data generated by the parametric HBMs. Nine sets of the thigh, the leg and the knee were isolated from the nine parametric HBMs. The thigh and the leg were subjected to lateral-to-medial mid-span dynamic 3-point bending to failure of the bones, while the knee was subjected to dynamic 4-point valgus bending to failure of the MCL. The maximum values of the BM were recorded for the thigh and the leg, while the maximum value of the knee valgus angle was obtained for the knee. Using the nine data for each of the lower limb components, virtual IPFs for human were developed by treating the data as exact data at failure and applying the Weibull survival analysis.

Next, TF was determined for each the thigh, the leg and the knee using one of the nine parametric HBMs that represents mean material property. The aPLI model developed in a pevious study[17] was also used. Since the aPLI does not represent failure of the tissues for repeatability, reproducibility and durability, the maximum value of an injury metric measured during an impact from a car may exceed the injury limits when an excessive load is applied. For this reason, failure representation of the HBM, except the fibula, was inactivated to correlate the maximum values of the injury metrics with those of the aPLI model under such conditions. Failure of the fibula was exceptionally activated so as to not underestimate loadings to the tibia, for which the injury metric is set for the aPLI. Thirty-six SCMs developed[17] were used to represent various load cases, with each of the 18 SCMs representing high-bumper and low-bumper cars. The aPLI model and the HBM were hit by each of the 36 SCMs in conformity to the STP. Specifically, the SCMs were made to collide with each of the HBM and the aPLI model in the lateral-to-medial direction at an impact speed of 11,1 m/s. As the bottom of the aPLI corresponds to the sole of a bare foot, the impact height of the aPLI model was set at 25 mm above the ground to compensate for the height of the sole of the shoe. As the length of the lower limb of the HBM is the same as that of the aPLI, and the mass of the shoe is combined with the foot model representing the shape of the bare foot, the impact height of the HBM was also set at 25 mm above the ground, as shown in Figure A.8. A gravity field is applied to the entire models. The lower limb orientation of the HBM was set such that the line connecting the centre of the hip joint and the ankle joint of the struck-side lower limb is vertical to the ground, and the same line on the non-struck side is rotated 20° forward about the hip joint, as shown in Figure A.9.

Injury metrics of the HBM and the aPLI model were measured at the locations illustrated in Figure A.10. The measurement locations on the femur and the tibia are labelled femur-1 through femur-3 and tibia-1 through tibia-4, respectively, in the ascending order from the location closest to the knee joint. The maximum values of the injury metrics for the thigh, the leg and the knee were recorded and used for regression analysis to develop virtual TFs. The BM was used as the injury metric for the femur and the tibia of the HBM and the aPLI model. In terms of the knee injury metric, the PMHS component tests to be used to develop the IPF for humans measure the knee valgus angle, rather than the elongation of the MCL, due to the need for the use of intact knees to ensure biofidelic response measurements. As the aPLI is capable of directly measuring elongation of the MCL, a transfer function was determined between the knee valgus angle of the HBM and the MCL elongation of the aPLI model. The femur BM and the tibia BM of the HBM were measured about the x-axis of the local coordinate system defined for each of the cross sections of the bones and affixed to the nodes comprising the solid elements that define the cross sections. The x-axis of all cross sections was initially oriented anteroposteriorly as shown in Figure A.10 in conformity to the BM measurement of the aPLI and FlexPLI.

The BM on the femur and the tibia/fibula of the HBM was measured by the section moment defined by the elements closest to the measurement locations of the aPLI. For the leg, the summation of the section moment on the tibia and the fibula was used for the assessment because these two bones are represented by a single bone core installed in the leg of the aPLI. The knee valgus angle was measured

© ISO 2023 – All rights reserved

AVA Documents Document Sharing Hub
Full document details: PD ISO/TS 20459:2023

by the local coordinate system defined at the knee-joint centre. The two nodes at the origin of the coordinate system were rigidly attached to the node on the femoral condyle and the tibial plateau with the closest proximity to these nodes to measure the angle of the tibia relative to the femur.

The femur BM and the tibia BM of the aPLI FE model were obtained by measuring the strain of the elements on the bone core closest to the measurement location of the aPLI hardware unit and converting it to bending moment using the sensitivity determined in a 3-point bending simulation of the bone core. The MCL elongation was directly measured by the elongation of the bar element simulating the MCL of the aPLI hardware.

The virtual TFs for the thigh and the leg were developed as linear regression functions with zero intercept determined between the maximum values of the BM obtained from the HBM and the aPLI model. In accordance with the STP, the maximum value of the BM was determined, for each the thigh and the leg, by the maximum of the maximum values obtained from multiple measurement locations (three and four locations on the femur and the tibia, similar to those of the aPLI). The virtual TF for the knee was developed by applying the same methodology as that used for the thigh and the leg, with the exception that the regression function was determined between different injury metrics (knee valgus angle for the HBM and the MCL elongation for the aPLI model).

Finally, the virtual IPFs for the aPLI were developed by applying the TFs determined above to the injury metrics for the HBM that define the virtual IPFs for human. Specifically, the virtual IPFs for the aPLI were determined using Formula (A.1):

$$\boldsymbol{P} = \boldsymbol{F}(\boldsymbol{I}_{\mathbf{human}}) = \boldsymbol{F}(\boldsymbol{G}(\boldsymbol{I}_{\mathbf{aPLI}})) \tag{A.1}$$

where

P is the probability of injury of human;

F is the IPF for human;

G is the transfer function;

I_{human} is the injury metric for human;

I_{aPLI} is the injury metric for the aPLI.

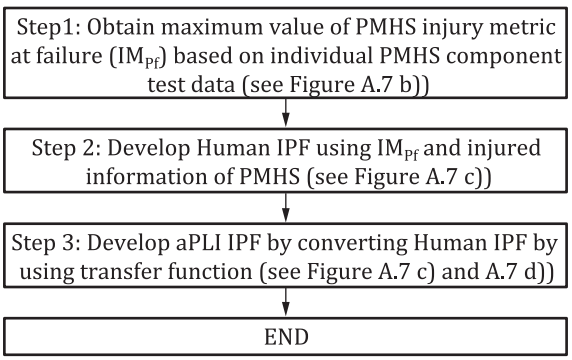

a) Flow chart for TF method

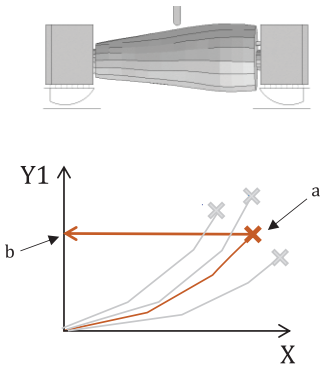

b) Schematic image of PMHS failure test and data

© ISO 2023 – All rights reserved
Documents
Document Sharing Hub
Full document details: PD ISO/TS 20459:2023

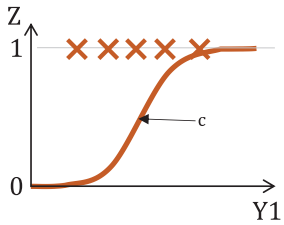

c) Schematic image of human IPF

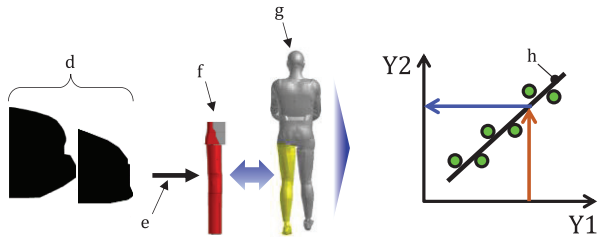

d) Schematic image of TF

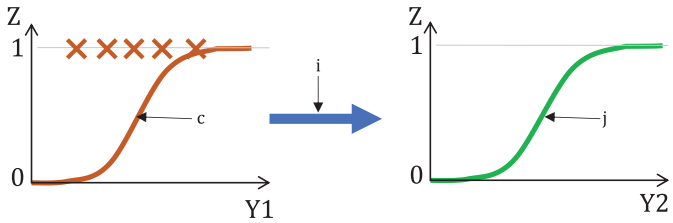

e) Schematic image of conversion

Key

X PMHS input (e.g. deflection)
Y1 PMHS injury metric
Y2 aPLI injury metric
Z human injury probability
a Injured.
b Maximum value of PMHS injury metric at failure (IM_{pf}).
c Human IPF.
d Car models.
e 11,1 m/s.
f aPLI model.
g HBM.
h TF (regression line).
i Conversion by using TF.
j aPLI IPF.

Figure A.7 — Development flow of IPF for human by means of the TF method

© ISO 2023 – All rights reserved

Documents
Document Sharing Hub
Full document details: PD ISO/TS 20459:2023

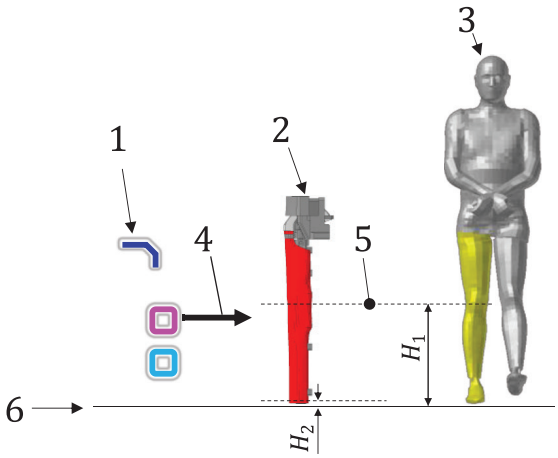

Key

1 SCM
2 aPLI FE model
3 HBM
4 11,1 m/s
5 knee joint
6 ground level
H_1 519 mm
H_2 25 mm

Figure A.8 — Setting of impact height of the HBM and the aPLI model

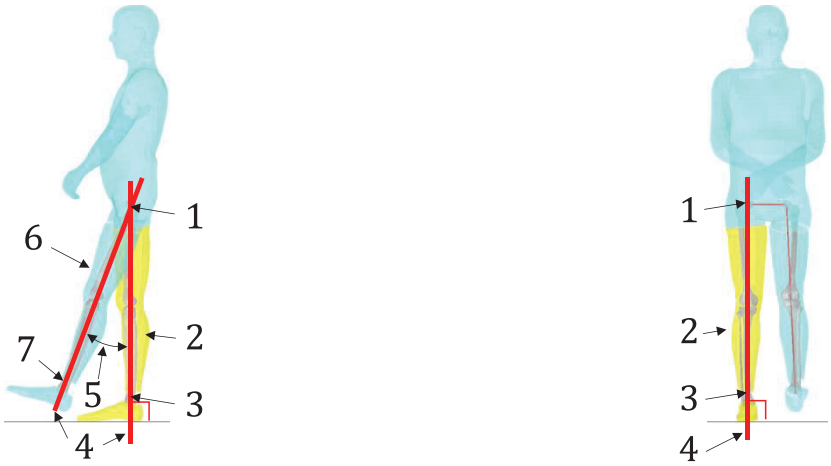

a) Struck-side view **b) Back view**

Key

1 hip-joint centre
2 struck side of vertical lower limb
3 ankle-joint centre
4 line connecting the centre of the hip joint and the ankle joint
5 20°
6 non-struck side of straight lower limb
7 ankle-joint centre

Figure A.9 — Lower-limb posture of the HBM

© ISO 2023 – All rights reserved
Documents
Document Sharing Hub
Full document details: PD ISO/TS 20459:2023

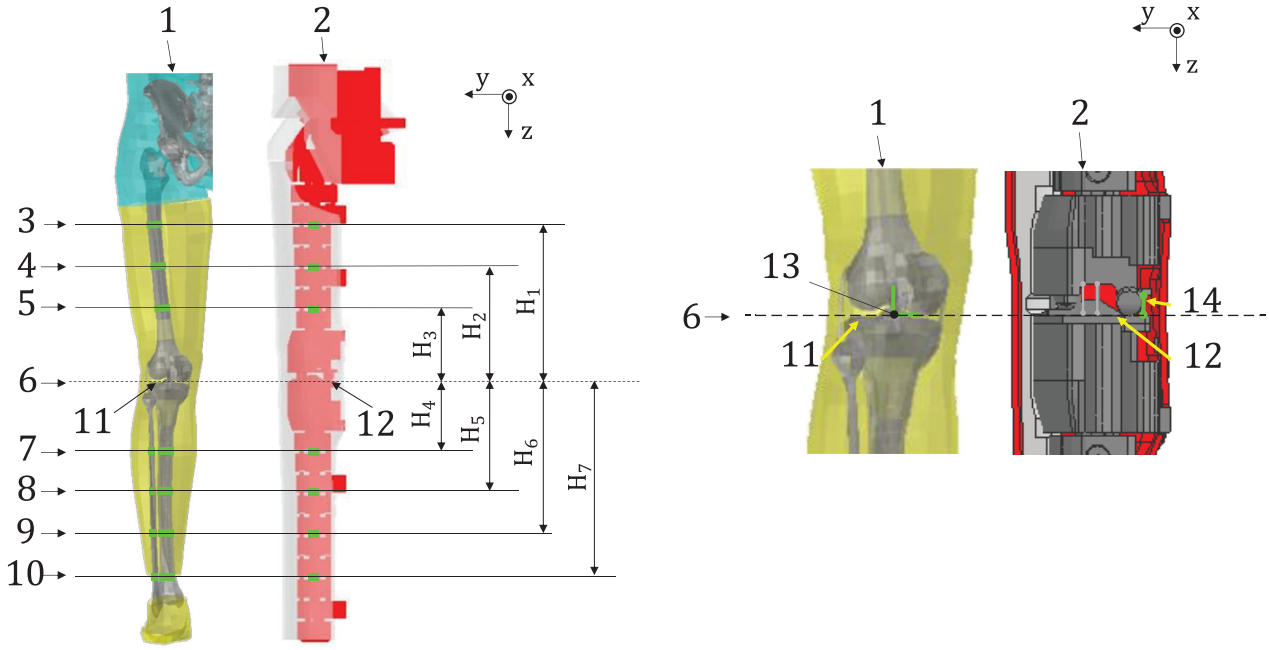

a) Long bones **b) Knee**

Key

1 HBM
2 aPLI FE model
3 BM measurement location (femur-3)
4 BM measurement location (femur-2)
5 BM measurement location (femur-1)
6 knee joint
7 BM measurement location (tibia-1)
8 BM measurement location (tibia-2)
9 BM measurement location (tibia-3)
10 BM measurement location (tibia-4)
11 tibial plateau
12 flat surface of tibial plateau
13 knee valgus angle measured at knee-joint centre
14 MCL elongation
H_1 297 mm
H_2 217 mm
H_3 137 mm
H_4 134 mm
H_5 214 mm
H_6 294 mm
H_7 374 mm

Figure A.10 — Measurement locations of the HBM and the aPLI model

A.2.2.2.3 Energy equivalent (EE) method

The assumption behind the EE method is that the deformation energy is the predictor of tissue failure. Given this assumption, injury occurrence is related to the aPLI injury value at the same deformation

© ISO 2023 – All rights reserved

Documents
Document Sharing Hub
Full document details: PD ISO/TS 20459:2023

energy as that absorbed by a human body up to the tissue failure. Component tests are used to establish this relationship due to the lack of sufficient full-scale pedestrian impact test data. For each individual human subject, a lower limb segment is subjected to a component test, such as a dynamic 3-point or 4-point test, and the deformation energy is calculated up to failure of the tissue. The same component test is performed using the corresponding aPLI segment, and the injury value at the same deformation energy is recorded. This develops a list of aPLI injury values corresponding to tissue failure of all the human subjects involved in the analysis. IPFs are determined by interpreting these injury values as those at failure. Figure A.11 shows a flow to develop IPFs for the aPLI using the EE method.

First, using the virtual biomechanical data generated by the parametric HBMs for the TF method as described in A.2.2.2.2, the deformation energy up to failure of the tissue (femur, tibia and MCL) was calculated for each of the nine parametric HBMs. The deformation energy up to failure was calculated by integrating the applied force in the 3-point bending simulation (thigh and leg) and the knee moment in the 4-point bending simulation (knee) with respect to the displacement of the indenter (thigh and leg) and the knee valgus angle (knee), respectively, from the initiation of the loading up to the initiation of the failure predicted by the HBM.

Second, each part of the lower limb (thigh, leg and knee) of the aPLI model was isolated, and dynamic 3-point bending simulation and dynamic 4-point bending simulation were performed with the thigh/leg and the knee, respectively, using the same boundary and loading conditions as those used for the HBM simulations. By applying the same methodology as that described above for the HBMs, the function defining the relationship between the injury value and the deformation energy was determined for the aPLI model for each of the injury metrics. For each combination of the nine parametric HBMs and the injury metrics, the aPLI injury value corresponding to the failure of the human tissue was determined by giving the deformation energy at failure obtained from the HBM to the function described above.

Finally, the resulting set of the nine aPLI injury values for each of the injury metrics was used to determine virtual IPF for the aPLI using the EE method by applying the Weibull survival analysis to each of the datasets and treating the data as exact.

© ISO 2023 – All rights reserved
Documents
Document Sharing Hub
Full document details: PD ISO/TS 20459:2023

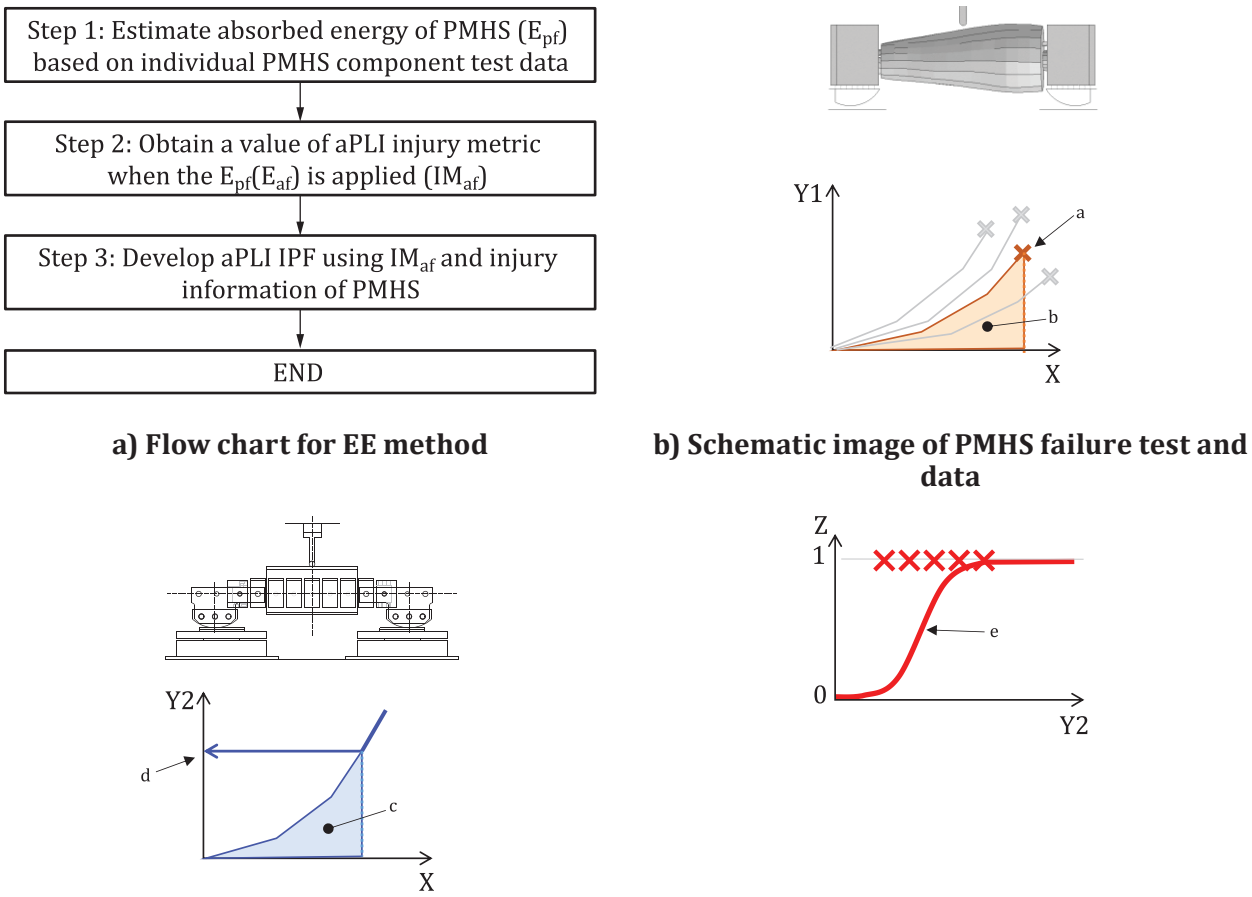

a) Flow chart for EE method

b) Schematic image of PMHS failure test and data

c) Schematic image of aPLI loading test and data

d) Schematic image of aPLI IPF

Key

X PMHS input (e.g. deflection)

Y1 PMHS injury metric

Y2 aPLI injury metric

Z human injury probability

a Injured.

b Estimated absorbed energy of PMHS (E_{pf}).

c Applied energy to aPLI (E_{af} = E_{pf}).

d A value of aPLI injury metric when the E_{pf} is applied (IM_{af}).

e aPLI IPF.

Figure A.11 — Development flow of IPF for human by means of the EE method

A.2.2.2.4 Paired test method

The paired test method (ISO/TR 12350) was used to derive IPFs for WorldSID, where full-scale human subjects and a full-scale dummy are subjected to an impact in the same loading condition, and IPFs for the dummy are derived by correlating occurrence of injuries to the human subjects and the maximum values of injury metrics for the specific body regions where the injuries occurred. Figure A.12 shows a flow to develop IPFs for the aPLI using the paired method.

First, the parametric HBMs and the aPLI model were subjected to impacts from SCMs. In order to develop reliable IPFs using the paired test method, the HBM impact simulations needed to provide data both

© ISO 2023 – All rights reserved

AVA Documents Document Sharing Hub
Full document details: PD ISO/TS 20459:2023

with injury and without injury, preferably with an even distribution, to a specific tissue (femur, tibia and MCL) to be assessed. Due to different tolerances and loading mechanisms of the tissues, different sets of nine SCMs needed to be used to obtain such data for the different tissues. The nine SCMs for the femur and the tibia were selected from the 36 SCMs[17] or 20 SCMs specified in A.2.4.2.2, while three modified SCMs as specified in Figure A.13, Figure A.14, Table A.2 and Table A.3 needed to be used, in addition to the six SCMs chosen from the set of 36 SCMs, to deliver impacts with no injury to the MCL. For the same reason, five impact speeds, with specific levels being different among different tissues, were also used. For each combination of the lower limb region and the impact speed, the combination of the nine SCMs and the nine parametric HBMs was randomly determined to reduce the number of simulation runs while maintaining evenly distributed probability of tissue failure. This resulted in 45 simulation runs for each of the lower limb regions. The simulation matrix is shown in Table A.1. In the table, the initial capital letter of the impact simulation case identifier denotes the specific lower limb region (T: thigh, L: leg, K: knee) for which an IPF was calculated using the data. The simplified car model identifier starting from either 'sedan' or 'SUV' are those selected from the set of 36 SCMs, while the identifier starting from 'Car' denotes the three modified SCMs specifically used for the knee. In addition, the human body model identifier corresponds to that described in A.2.2.2.1. The impact simulation setup, except impact speed, is the same as described in A.2.2.2.2. The aPLI model was subjected to impacts in all of the 135 load cases listed in Table A.1.

Next, the maximum values of the injury metrics of the aPLI model were linked with the occurrence of injury (with/without injury) predicted by the corresponding HBM impact simulations. Since the aPLI does not simulate failure of tissues and injury values may read beyond the tolerance of the tissues, aPLI injury values corresponding to 'injury' and 'no injury' were treated as left censored data and right censored data, respectively. The virtual IPFs for the aPLI using the paired method were developed by means of the Weibull survival analysis.

© ISO 2023 – All rights reserved
Documents
Document Sharing Hub
Full document details: PD ISO/TS 20459:2023

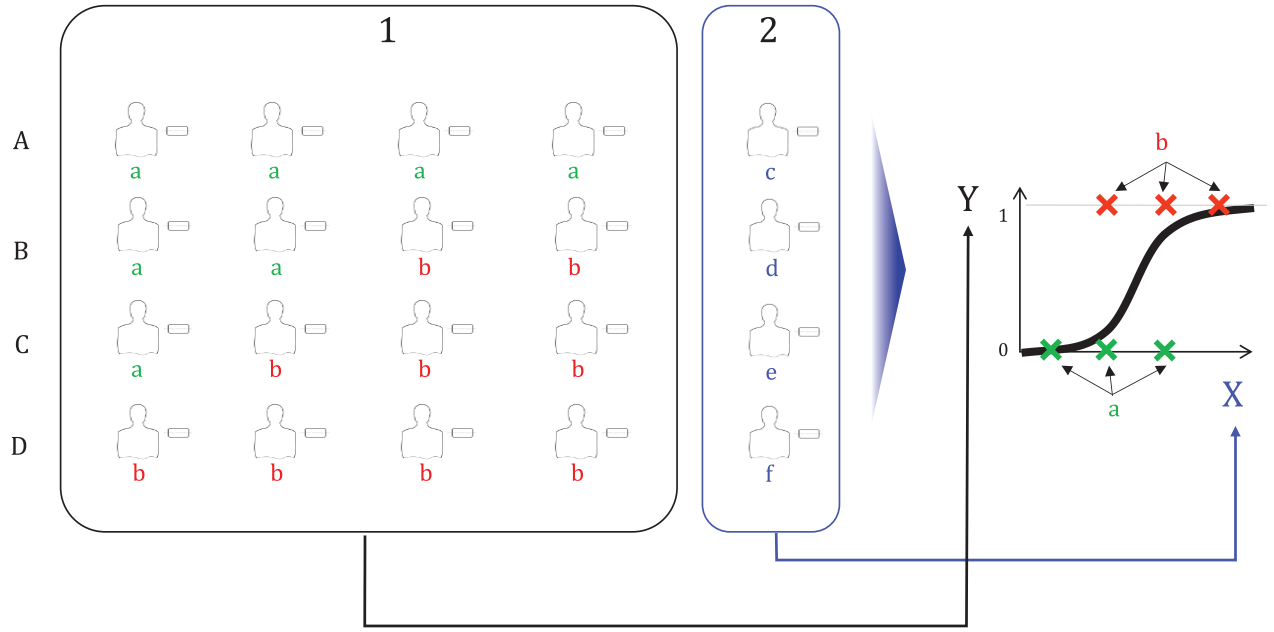

Key

X ATD injury metrics (e.g. force)
Y human injury probability
1 PMHS test
2 ATD test
A load case (A)
B load case (B)
C load case (C)
D load case (D)
[a] Intact.
[b] Injury.
[c] A value of ATD injury metric observed in load case (A).
[d] A value of ATD injury metric observed in load case (B).
[e] A value of ATD injury metric observed in load case (C).
[f] A value of ATD injury metric observed in load case (D).

Figure A.12 — Development Flow of IPF for human by means of the paired test method

Table A.1 — HBM impact simulation matrix for the virtual paired test method

Case	S	SCM	HBM	Case	S	SCM	HBM	Case	S	SCM	HBM
T-1	30	J-SDN-13	HBM-3	L-1	30	Sedan12	HBM-3	K-1	10	Car-PC	HBM-3
T-2	30	SUV09	HBM-9	L-2	30	SUV11	HBM-9	K-2	10	Sedan08	HBM-9
T-3	30	SUV11	HBM-4	L-3	30	SUV01	HBM-4	K-3	10	Sedan18	HBM-4
T-4	30	J-LoBP-SUV-09	HBM-8	L-4	30	Sedan17	HBM-8	K-4	10	Car-PA	HBM-8
T-5	30	J-SDN-10	HBM-2	L-5	30	Sedan05	HBM-2	K-5	10	Sedan07	HBM-2

Key

Case impact simulation case identifier
S impact speed [km/h]
SCM simplified car model identifier
HBM human body model identifier

© ISO 2023 – All rights reserved

Documents
Document Sharing Hub
Full document details: PD ISO/TS 20459:2023

Table A.1 *(continued)*

Case	S	SCM	HBM	Case	S	SCM	HBM	Case	S	SCM	HBM
T-6	30	J-SDN-02	HBM-7	L-6	30	Sedan08	HBM-7	K-6	10	Car-PB	HBM-7
T-7	30	Sedan12	HBM-1	L-7	30	SUV02	HBM-1	K-7	10	Sedan06	HBM-1
T-8	30	SUV05	HBM-5	L-8	30	SUV04	HBM-5	K-8	10	Sedan10	HBM-5
T-9	30	J-SDN-14	HBM-6	L-9	30	SUV15	HBM-6	K-9	10	Sedan11	HBM-6
T-10	40	J-SDN-02	HBM-3	L-10	40	Sedan08	HBM-3	K-10	20	Car-PB	HBM-3
T-11	40	J-SDN-14	HBM-1	L-11	40	SUV15	HBM-1	K-11	20	Sedan11	HBM-1
T-12	40	SUV09	HBM-2	L-12	40	SUV11	HBM-2	K-12	20	Sedan08	HBM-2
T-13	40	Sedan12	HBM-8	L-13	40	SUV02	HBM-8	K-13	20	Sedan06	HBM-8
T-14	40	SUV05	HBM-7	L-14	40	SUV04	HBM-7	K-14	20	Sedan10	HBM-7
T-15	40	J-LoBP-SUV-09	HBM-6	L-15	40	Sedan17	HBM-6	K-15	20	Car-PA	HBM-6
T-16	40	SUV11	HBM-5	L-16	40	SUV01	HBM-5	K-16	20	Sedan18	HBM-5
T-17	40	J-SDN-13	HBM-9	L-17	40	Sedan12	HBM-9	K-17	20	Car-PC	HBM-9
T-18	40	J-SDN-10	HBM-4	L-18	40	Sedan05	HBM-4	K-18	20	Sedan07	HBM-4
T-19	50	Sedan12	HBM-3	L-19	50	SUV02	HBM-3	K-19	30	Sedan06	HBM-3
T-20	50	SUV09	HBM-5	L-20	50	SUV11	HBM-5	K-20	30	Sedan08	HBM-5
T-21	50	J-SDN-02	HBM-9	L-21	50	Sedan08	HBM-9	K-21	30	Car-PB	HBM-9
T-22	50	J-SDN-14	HBM-8	L-22	50	SUV15	HBM-8	K-22	30	Sedan11	HBM-8
T-23	50	J-LoBP-SUV-09	HBM-4	L-23	50	Sedan17	HBM-4	K-23	30	Car-PA	HBM-4
T-24	50	SUV11	HBM-7	L-24	50	SUV01	HBM-7	K-24	30	Sedan18	HBM-7
T-25	50	J-SDN-10	HBM-2	L-25	50	Sedan05	HBM-2	K-25	30	Sedan07	HBM-2
T-26	50	J-SDN-13	HBM-1	L-26	50	Sedan12	HBM-1	K-26	30	Car-PC	HBM-1
T-27	50	SUV05	HBM-6	L-27	50	SUV04	HBM-6	K-27	30	Sedan10	HBM-6
T-28	60	SUV11	HBM-6	L-28	60	SUV01	HBM-6	K-28	40	Sedan18	HBM-6
T-29	60	Sedan12	HBM-4	L-29	60	SUV02	HBM-4	K-29	40	Sedan06	HBM-4
T-30	60	J-SDN-13	HBM-9	L-30	60	Sedan12	HBM-9	K-30	40	Car-PC	HBM-9
T-31	60	J-SDN-14	HBM-3	L-31	60	SUV15	HBM-3	K-31	40	Sedan11	HBM-3
T-32	60	J-LoBP-SUV-09	HBM-7	L-32	60	Sedan17	HBM-7	K-32	40	Car-PA	HBM-7
T-33	60	SUV09	HBM-2	L-33	60	SUV11	HBM-2	K-33	40	Sedan08	HBM-2
T-34	60	SUV05	HBM-1	L-34	60	SUV04	HBM-1	K-34	40	Sedan10	HBM-1
T-35	60	J-SDN-02	HBM-8	L-35	60	Sedan08	HBM-8	K-35	40	Car-PB	HBM-8
T-36	60	J-SDN-10	HBM-5	L-36	60	Sedan05	HBM-5	K-36	40	Sedan07	HBM-5
T-37	70	J-LoBP-SUV-09	HBM-2	L-37	70	Sedan17	HBM-2	K-37	50	Car-PA	HBM-2
T-38	70	Sedan12	HBM-1	L-38	70	SUV02	HBM-1	K-38	50	Sedan06	HBM-1
T-39	70	SUV05	HBM-8	L-39	70	SUV04	HBM-8	K-39	50	Sedan10	HBM-8
T-40	70	J-SDN-10	HBM-3	L-40	70	Sedan05	HBM-3	K-40	50	Sedan07	HBM-3
T-41	70	J-SDN-13	HBM-7	L-41	70	Sedan12	HBM-7	K-41	50	Car-PC	HBM-7
T-42	70	J-SDN-02	HBM-4	L-42	70	Sedan08	HBM-4	K-42	50	Car-PB	HBM-4
T-43	70	J-SDN-14	HBM-9	L-43	70	SUV15	HBM-9	K-43	50	Sedan11	HBM-9
T-44	70	SUV09	HBM-5	L-44	70	SUV11	HBM-5	K-44	50	Sedan08	HBM-5

Key

Case	impact simulation case identifier
S	impact speed [km/h]
SCM	simplified car model identifier
HBM	human body model identifier

© ISO 2023 – All rights reserved

Documents
Document Sharing Hub

Full document details: PD ISO/TS 20459:2023

Table A.1 *(continued)*

Case	S	SCM	HBM	Case	S	SCM	HBM	Case	S	SCM	HBM
T-45	70	SUV11	HBM-6	L-45	70	SUV01	HBM-6	K-45	50	Sedan18	HBM-6

Key

Case	impact simulation case identifier
S	impact speed [km/h]
SCM	simplified car model identifier
HBM	human body model identifier

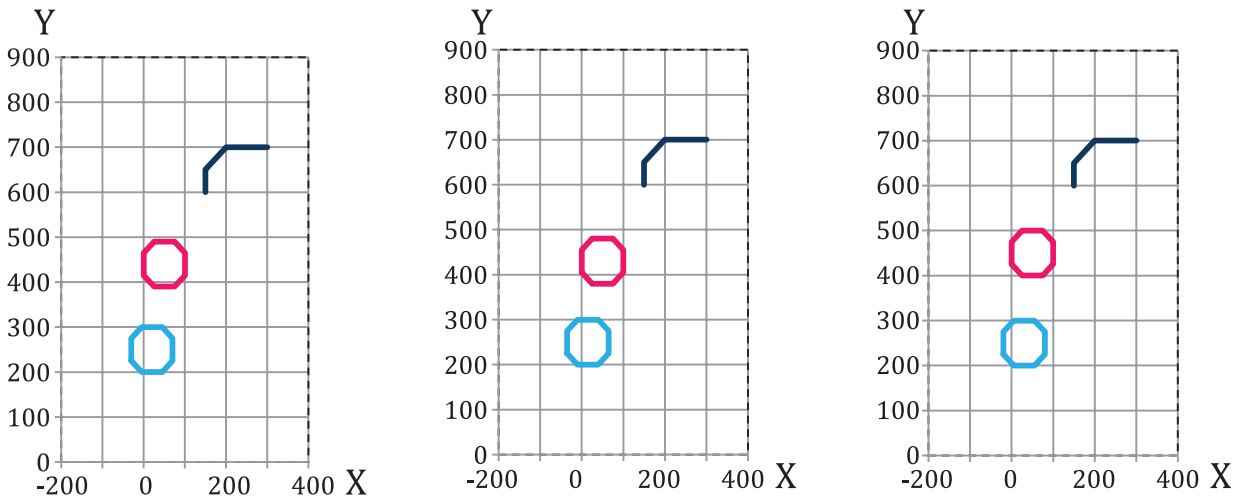

a) Car-PA **b) Car-PB** **c) Car-PC**

Key

X horizontal dimensions [mm]

Y vertical dimensions [mm]

Figure A.13 — Geometry of additional SCMs (car-PA, car-PB and car-PC) to develop a virtual IPF for the knee by using the pared test method

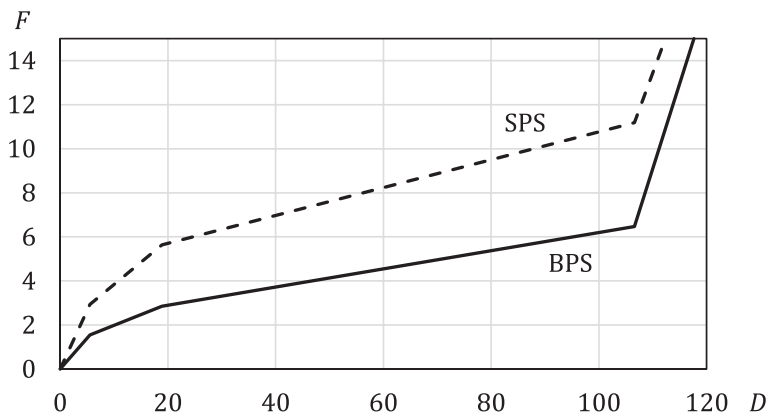

a) Bumper and spoiler stiffness

© ISO 2023 – All rights reserved

Documents
Document Sharing Hub
Full document details: PD ISO/TS 20459:2023

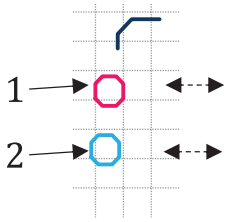

b) Direction of deflection

Key

1	bumper
2	spoiler
F	force [kN]
D	deflection [mm]
BPS	bumper stiffness curve specified for car-PA, car-PB and car-PC
SPS	spoiler stiffness curve specified for car-PA, car-PB and car-PC

Figure A.14 — Stiffness curves specified for the bumper and spoiler of the three SCMs (car-PA, car-PB, car-PC)

Table A.2 — Tabulated geometry data of three SCMs (car-PA, car-PB, car-PC)

SCM ID	Dimensions in millimeters				
	H1	H2	H3	L1	L2
Car-PA	700	440	250	200	-30
Car-PB	700	430	250	200	-35
Car-PC	700	450	250	200	-20

Key

1	bonnet leading edge (BLE)
2	bumper (BP)
3	spoiler (SP)
H1	BLE height
H2	bumper centre height
H3	spoiler centre height
L1	bonnet lead
L2	SP lead

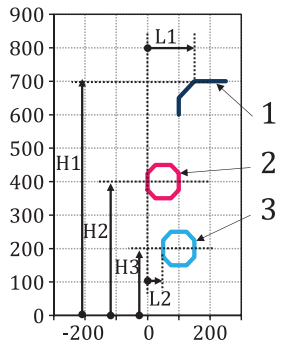

Table A.3 — Tabulated stiffness data specified for bumper and spoiler of three SCMs (car-PA, car-PB, car-PC)

Bumper		Spoiler	
D	F	D	F
0,0	0	0,0	0

Key

D	deflection [mm]
F	force [kN]
BP	bumper stiffness curve specified for car-PA, car-PB and car-PC
SP	spoiler stiffness curve specified for car-PA, car-PB and car-PC

© ISO 2023 – All rights reserved
Documents
Document Sharing Hub
Full document details: PD ISO/TS 20459:2023

Table A.3 *(continued)*

Bumper		Spoiler	
D	F	D	F
5,6	1,5	5,6	2,9
18,9	2,9	18,9	5,6
106,6	6,5	106,6	11,2
150,0	40,0	150,0	40,0

Key

D deflection [mm]

F force [kN]

BP bumper stiffness curve specified for car-PA, car-PB and car-PC

SP spoiler stiffness curve specified for car-PA, car-PB and car-PC

A.2.2.3 Assessment of methods

Due to the lack of suitable and sufficient biomechanical data, an alternative methodology to develop the IPFs for the aPLI to the paired test method described in ISO/TR 12350 needed to be defined. In order to select one of the proposed methodologies (TF method or EE method), biomechanical data were virtually generated to develop IPFs using the three methods (TF method, EE method and paired test method) as described in A.2.2.2, and the IPFs determined using the TF method and the EE method were compared against the IPFs calculated using the paired test method to identify the methodology that provides the IPFs that better represent those from the paired test method.

The use of the EE method described in A.2.3.2.3 requires calculation of the deformation energy from the biomechanical data, while the TF method requires only the maximum values of the injury metrics as described in A.2.2.2.2. For this reason, the availability of sufficient data from that literature was also analysed.

A.2.2.3.1 Assessment against virtual paired test method

Figure A.15 through Figure A.17 shows the comparison of the virtual IPFs for the aPLI developed by using the TF method, EE method and paired test method. The virtual IPFs developed by using the TF method better represent those of the paired test method than that developed using the EE method. The normalized errors of the injury value at 50 % probability of injury relative to the IPF developed using the paired test method were 12,1 %, 1,0 % and 0,5 % for the TF method, and 23,1 %, 21,0 % and 7,4 % for the EE method, for the thigh, the leg and the knee, respectively. These results indicate that use of the TF method is recommended as an alternative method to the paired test method recommended by ISO.

Note that the reliability of the conclusion depends on the validity of the baseline and parametric HBMs used in this analysis. See Tables A.5 and A.6 for the parameters of virtual aPLI IPF for the MCL complete rupture and for the femus shaft (Weibull distribution).

© ISO 2023 – All rights reserved

Documents
Document Sharing Hub
Full document details: PD ISO/TS 20459:2023

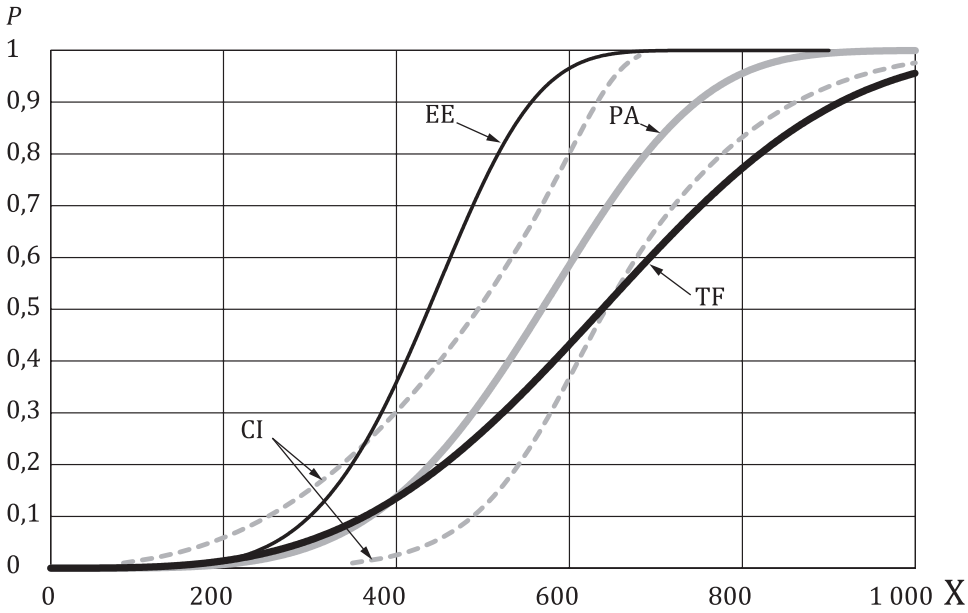

Key

X aPLI femur BM [Nm]

P probability of femur shaft fracture

TF virtual aPLI IPF for femur shaft fracture developed by using TF method

EE virtual aPLI IPF for femur shaft fracture developed by using EF method

PA virtual aPLI IPF for femur shaft fracture developed by using paired test method

CI 95 % confidence interval

Figure A.15 — Virtual aPLI IPFs for the femur shaft fracture developed by using the TF method, EE method and paired test method

Table A.4 — Parameters of virutal aPLI IPF for the femur shaft (Wibull distribution)

Deveopment method	C_{Scale}	C_{Shape}
TF	711	3,35
EE	470	4,99
Paired	618	4,39

© ISO 2023 – All rights reserved

Documents
Document Sharing Hub

Full document details: PD ISO/TS 20459:2023

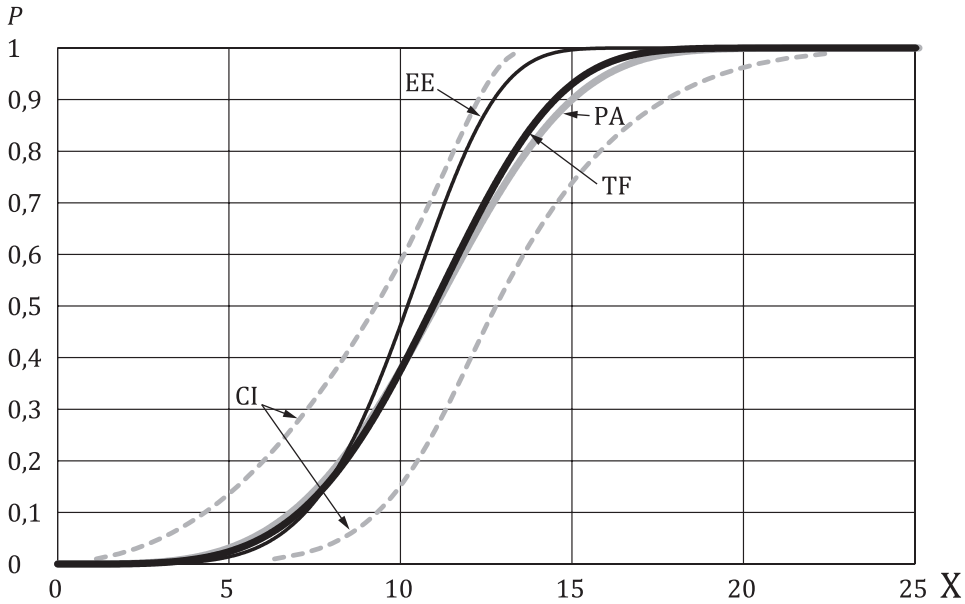

Key

Y aPLI MCL elongation [mm]

P probability of MCL complete rupture

TF virtual aPLI IPF for MCL complete rupture developed by using TF method

EE virtual aPLI IPF for MCL complete rupture developed by using EE method

PA virtual aPLI IPF for MCL complete rupture developed by using paired test method

CI 95 % confidence interval

Figure A.16 — Virtual aPLI IPFs for the MCL complete rupture developed by using the TF method, EE method and paired test method

Table A.5 — Parameters of virtual aPLI IPF for the MCL complete rupture (Weibull distribution)

Development method	C_{Scale}	C_{Scale}
TF	12,0	4,27
EE	10,9	5,45
Paired	12,1	3,90

© ISO 2023 – All rights reserved

Documents
Document Sharing Hub
Full document details: PD ISO/TS 20459:2023

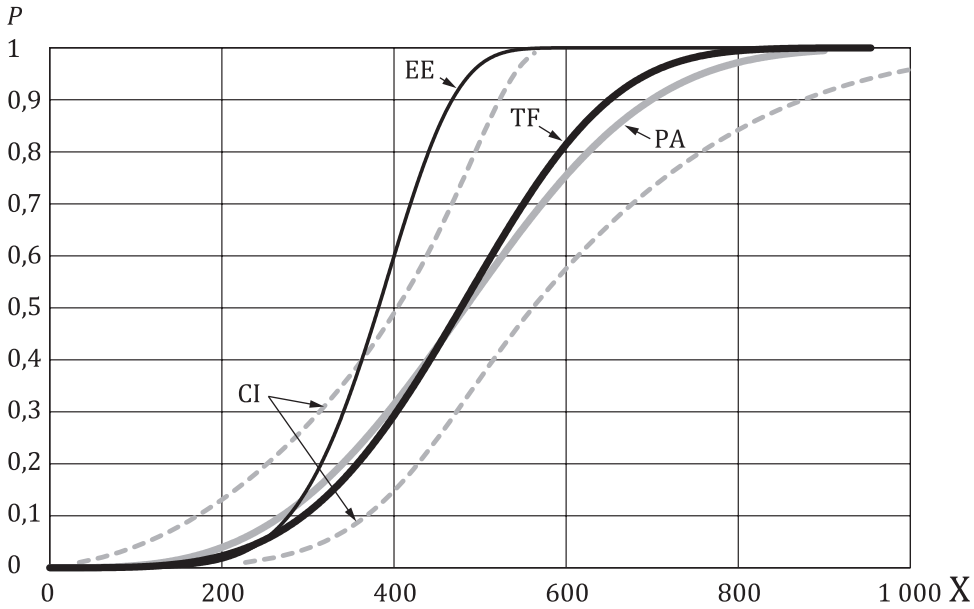

Key

X aPLI tibia BM [Nm]

P probability of tibia shaft fracture

TF virtual aPLI IPF for tibia shaft fracture developed by using TF method

EE virtual aPLI IPF for tibia shaft fracture developed by using EE method

PA virtual aPLI IPF for tibia shaft fracture developed by using paired test method

CI 95 % confidence interval

Figure A.17 — Virtual aPLI IPFs for the tibia shaft fracture developed by using the TF method, EE method and paired test method

Table A.6 — Parameters of virtual aPLI IPF for the femur shaft (Weibull distribution)

Development Method	C_{Scale}	C_{Shape}
TF	525	3,90
EE	406	5,92
Paired	540	3,24

A.2.2.3.2 Assessment of number of biomechanical data

Table A.7 summarizes the availability of maximum values of injury metrics used for the TF method, and the availability of diagrams (BM – indenter displacement for the thigh/leg, BM - valgus angle for the knee) used for the EE method, from the literature (see [13], [15], [14], [16], [18], [19], [20], [21], [22] and [23]). The number of available data is significantly smaller for those with diagrams.

© ISO 2023 – All rights reserved

Documents
Document Sharing Hub
Full document details: PD ISO/TS 20459:2023

Table A.7 — Availability of maximum values of injury metrics and diagrams from the literature

Body region	Reference	Number of tests	
		Maximum value of injury metrics	Diagram
Thigh	Kerrigan et al. (2003a)	4	1
	Kerrigan et al. (2004)	6	6
	Funk et al. (2004)	15	0
	Ivarsson et al. (2009)	10	10
	Total	35	17
Leg	Nyquist et al. (1985)	9	0
	Kerrigan et al. (2003a)	4	1
	Kerrigan et al. (2003b)	6	0
	Kerrigan et al. (2004)	4	4
	Total	23	5
Knee	Kajzer et al. (1997)	9	0
	Kajzer et al. (1999)	3	0
	Bose et al. (2004)	8	8
	Bose et al. (2008)	8	0
	Total	28	8

A.2.2.3.3 Conclusions

Based on the results of A.2.2.3.1 and A.2.2.3.2 discussed at the 9th aPLI TG meeting in London, the aPLI TG decided to use the TF method.

A.2.3 Development of IPFs for human

A.2.3.1 General

Biomechanical data consistent with the load case under which the subsystem test is performed with the aPLI were taken from the literature. In terms of the anthropometry, the height and the weight of human subjects were used as covariates in the statistical prediction modelling to control for a 50th percentile male represented by the aPLI.[3] In addition, the age was also controlled for the average age of all the subjects used in the experiments from which human biomechanical data were obtained (see Annex A.2.3.3). Only the past studies where these anthropometric parameters are specified were referenced. Data were collected from the studies that dynamically tested the isolated thigh and/or the leg (femur and/or tibia/fibula surrounded by the flesh and the skin) in the lateral-medial 3-point bending, and the studies that dynamically tested the intact knee in valgus bending. In addition, the injury metrics specified in the scope of the IPFs (femur and tibia BM, knee valgus angle; see Annex A.2.3.3.1) needed to be measured by the studies. The statistical procedure described in ISO/TS 18506 was employed to establish statistical prediction models.

A.2.3.2 Statistical prediction modelling

In the statistical prediction modelling, survival analysis was used to determine the injury probability function, with the height, the weight and the age of a subject defined as covariates.

With regard to data censoring, injury and intact (no injury) data were treated as exact and right censored data, respectively. In cases where a low-pass filter was applied, data were treated as right censored data due to attenuation of the maximum values. Data for the femur and the tibia obtained from the experiments using the specimens without the flesh were treated as right censored data considering the reduction of the maximum values due to the lack of load distribution provided by the flesh[14].

© ISO 2023 – All rights reserved

Documents
Document Sharing Hub
Full document details: PD ISO/TS 20459:2023

Within the three distributions recommended by ISO/TS 18506, one of the three distributions (Weibull distribution, Log-Normal distribution and Log-Logistic distribution; best fit to data) is used to define human IPFs for each of the injury metrics based on the score of Akaike's information criterion (AIC). The smallest score of the AIC means the best fit to data. The formulae of the human IPFs for these distributions are presented below.

The injury probability when the Weibull distribution is applied [Formula (A.2)]:

$$P = 1 - \exp\left\{-\left(\frac{x_{\text{human}}}{C_{\text{Scale}}}\right)^{C_{\text{Shape}}}\right\} \tag{A.2}$$

where

P is the injury probability of human;

C_{Scale} is the parameter determined for the Weibull distribution for human IPFs;

C_{Shape} is the parameter determined for the Weibull distribution for human IPFs;

C_{Slope} is the slope of the transfer function (TF);

x_{human} is the value of the injury metric for human.

The injury probability when the Log-Normal distribution is applied [Formula (A.3)]:

$$P = \frac{1}{C_{\sigma}\sqrt{2\pi}}\int_{0}^{x_{\text{human}}} \frac{1}{t}\exp\left\{\frac{-\left(\ln t - C_{\mu}\right)^{2}}{2C_{\sigma}^{2}}\right\}\mathrm{d}t \tag{A.3}$$

where

P is the injury probability of human;

C_{μ} is the parameter determined for the Log-Normal distribution for human IPFs;

C_{σ} is the parameter determined for the Log-Normal distribution for human IPFs;

C_{Slope} is the slope of the TF;

x_{human} is the value of the injury metric for human.

The injury probability when the Log-Logistic distribution is applied [Formula (A.4)]:

$$P = \frac{1}{1 + \left(\frac{x_{\text{human}}}{\exp\left(C_{\text{Scale}}\right)}\right)^{\frac{-1}{C_{\text{Shape}}}}} \tag{A.4}$$

where

P is the injury probability of human;

C_{Scale} is the parameter determined for the Log-Logistic distribution for human IPFs;

C_{Shape} is the parameter determined for the Log-Logistic distribution for human IPFs;

C_{Slope} is the slope of the TF;

x_{human} is the value of the injury metric for human.

© ISO 2023 – All rights reserved
Documents
Document Sharing Hub
Full document details: PD ISO/TS 20459:2023

A.2.3.3 Biomechanical data

A.2.3.3.1 Data collection

Human biomechanical data obtained from past experimental studies were collected from the literature. The following inclusion criteria were set to generate IPFs for human consistent with the conditions and the load case specified by the STP under which aPLI car tests are performed:

— regions of the lower limb: thigh, leg and knee;

— specific injuries reproduced: femur shaft fracture, tibia shaft fracture and MCL complete rupture;

— injury metrics: thigh BM, tibia BM and knee valgus angle;

— loading rate: equivalent to a 11,1 m/s car-pedestrian collision;

— loading direction: lateral-to-medial, anterior-to-posterior and posterior-to-anterior for the thigh and lateral-to-medial for the leg and the knee;

— lower-limb posture: fully-extended knee.

In addition to the lateral-to-medial loading direction (STP loading direction), posterior-to-anterior and anterior-to-posterior loading direction were also accepted for the thigh because the bending tolerance of the thigh is not sensitive to the loading direction due to the circular cross-sectional shape of the femoral shaft[23]).

The IPFs for the aPLI shall be developed for the thigh, leg and knee that comprises a human lower limb for which the aPLI measures injury values.

Femur shaft fracture, tibia shaft facture and MCL complete rupture were selected because these are the primary injuries to the three lower limb regions specified (References [8] and [24]). Although not necessarily frequent compared to bone fractures, MCL failure was included considering long-term consequences of the injury[25]. Failure of the ACL and PCL were not included because isolated failure of these ligaments is rare in pedestrian accidents[26] and is typically accompanied by MCL failure[16]. Bending moment was used as an injury metric for femur fracture and tibia fracture because bending moment was found to be the best predictor of those injuries in car-pedestrian impacts[27]. MCL elongation was chosen because failure of ligaments was found to be solely determined by the ultimate strain[28],[29]. Due to the lack of biomechanical data for MCL elongation, the knee valgus angle was used to describe the IPF for the human knee as the knee valgus angle determines the elongation of the MCL in lateral bending of the knee that occurs in a lateral impact specified in the STP.

The load case for which IPFs for human are to be developed followed that specified by the STP. The loading rate of a component shall be equivalent to the impact speed of 11,1 m/s. The impact direction shall be the lateral-to-medial direction to a pedestrian lower limb, and the knee shall be fully extended, to represent the load case specified in the STP.

In order to eliminate outliers, the dfbetas statistics defined in ISO/TS 18506 with the cut-off value of 0,3 were applied to identify overly influential observations in the collected biomechanical data.

A.2.3.3.2 Thigh

Table A.8 shows the collected biomechanical data for the thigh available from literature (see References [13], [14], 18] and [19]).

Potential overly influential PMHS test data (ID: 1-1, 1-4, 1-7, 1-8, 1-10, 1-13) were identified using the dfbetas statistics (Dfbetas > 0,3) as specified in ISO/TS 18506. IPFs with the identified data excluded one by one from the dataset were developed as shown in D.1.1. This resulted in the range of the injury values at the 50 % probability of injury being average ±4,0 %, compared to the range of confidence intervals of ±8,6 %. As the influence of the identified data was found to be not significant, all the PMHS data were used to develop the IPF.

© ISO 2023 – All rights reserved

Documents
Document Sharing Hub
Full document details: PD ISO/TS 20459:2023

Table A.8 — Biomechanical data for the thigh

Reference	ID	Age (YO)	Gender	Body mass [kg]	Stature [cm]	Flesh	Loading direction	Test type	BM [Nm]	Injury occurrence	Censoring	POI
Kerrigan et al. (2003)	1-1	55	M	85,0	172,7	Without	LM	D-3PB	632,5	Yes	RC	Yes
Kerrigan et al. (2003)	1-2	59	F	79,0	167,6	Without	LM	D-3PB	362,3	Yes	RC	No
Kerrigan et al. (2003)	1-3	54	F	50,0	162,6	Without	LM	D-3PB	340,0	Yes	RC	No
Kerrigan et al. (2003)	1-4	54	F	50,0	162,6	With	LM	D-3PB	376,7	Yes	EX	Yes
Kerrigan et al. (2004)	1-5	66	M	79,8	182,9	With	LM	D-3PB	548,0	Yes	EX	No
Kerrigan et al. (2004)	1-6	69	M	81,6	170,2	With	LM	D-3PB	568,0	Yes	EX	No
Kerrigan et al. (2004)	1-7	65	M	118,8	172,7	With	LM	D-3PB	640,0	Yes	EX	Yes
Kerrigan et al. (2004)	1-8	54	M	87,5	190,5	With	LM	D-3PB	424,0	Yes	EX	Yes
Kerrigan et al. (2004)	1-9	69	M	83,9	172,7	With	LM	D-3PB	488,0	Yes	EX	No
Kerrigan et al. (2004)	1-10	54	M	117,9	188,0	With	LM	D-3PB	685,0	Yes	EX	Yes
Funk et al. (2004)	1-11	67	M	64,0	188,0	Without	PA	D-3PB	355,0	Yes	RC	No
Funk et al. (2004)	1-12	59	M	108,0	182,9	Without	PA	D-3PB	593,0	Yes	RC	No
Funk et al. (2004)	1-13	40	M	70,0	180,3	Without	PA	D-3PB	605,0	Yes	RC	Yes
Funk et al. (2004)	1-14	55	M	64,0	167,6	Without	PA	D-3PB	363,0	Yes	RC	No
Funk et al. (2004)	1-15	70	M	73,0	167,6	Without	PA	D-3PB	359,0	Yes	RC	No
Funk et al. (2004)	1-16	69	M	92,0	162,6	Without	PA	D-3PB	460,0	Yes	RC	No
Funk et al. (2004)	1-17	51	M	124,0	188,0	Without	PA	D-3PB	599,0	Yes	RC	No
Funk et al. (2004)	1-18	66	M	95,0	182,9	Without	PA	D-3PB	373,0	Yes	RC	No
Funk et al. (2004)	1-19	67	M	64,0	188,0	Without	LM	D-3PB	435,0	Yes	RC	No
Funk et al. (2004)	1-20	59	M	108,0	182,9	Without	LM	D-3PB	497,0	Yes	RC	No
Funk et al. (2004)	1-21	40	M	70,0	180,3	Without	LM	D-3PB	528,0	Yes	RC	No
Funk et al. (2004)	1-22	55	M	64,0	167,6	Without	LM	D-3PB	389,0	Yes	RC	No
Funk et al. (2004)	1-23	70	M	73,0	167,6	Without	LM	D-3PB	356,0	Yes	RC	No
Funk et al. (2004)	1-24	69	M	92,0	162,6	Without	LM	D-3PB	419,0	Yes	RC	No
Funk et al. (2004)	1-25	51	M	124,0	188,0	Without	LM	D-3PB	543,0	Yes	RC	No
Ivarsson et al. (2009)	1-26	52	F	45,0	162,6	Without	AP	D-3PB	120,0	Yes	RC	No
Ivarsson et al. (2009)	1-27	52	F	45,0	162,6	Without	PA	D-3PB	147,0	Yes	RC	No
Ivarsson et al. (2009)	1-28	63	M	89,0	180,3	Without	PA	D-3PB	422,0	Yes	RC	No
Ivarsson et al. (2009)	1-29	62	F	90,7	170,2	Without	AP	D-3PB	364,0	Yes	RC	No
Ivarsson et al. (2009)	1-30	62	F	90,7	170,2	Without	AP	D-3PB	440,0	Yes	RC	No
Ivarsson et al. (2009)	1-31	45	M	68,1	175,3	Without	PA	D-3PB	238,0	Yes	RC	No
Ivarsson et al. (2009)	1-32	45	M	68,1	175,3	Without	AP	D-3PB	381,0	Yes	RC	No
Ivarsson et al. (2009)	1-33	39	M	79,4	184,0	Without	PA	D-3PB	433,0	Yes	RC	No
Ivarsson et al. (2009)	1-34	51	M	54,9	175,0	Without	AP	D-3PB	343,0	Yes	RC	No
Ivarsson et al. (2009)	1-35	57	F	108,9	165,0	Without	PA	D-3PB	193,0	Yes	RC	No

Key

YO	years-old
M	male
F	female
LM	lateral to medial
AP	anterior to posterior
PA	posterior to anterior
D-3PB	dynamic 3-point bending test
RC	right censored
EX	exact
POI	potential overly influential observation

© ISO 2023 – All rights reserved
Documents
Document Sharing Hub
Full document details: PD ISO/TS 20459:2023